

# General expressions for internal deformation due to a moment tensor in an elastic/viscoelastic multilayered half-space

Akinori Hashima,<sup>1</sup> Youichiro Takada,<sup>2</sup> Yukitoshi Fukahata<sup>1</sup> and Mitsuhiro Matsu'ura<sup>1</sup>

<sup>1</sup>Department of Earth and Planetary Science, University of Tokyo, 7-3-1 Hongo, Bunkyo-ku, Tokyo 113-0033, Japan. E-mail: ahash@eps.s.u-tokyo.ac.jp

<sup>2</sup>Department of Earth Sciences, University of Oxford, Oxford, UK

Accepted 2008 April 28. Received 2008 March 27; in original form 2007 February 20

## SUMMARY

In the framework of elasticity theory any indigenous source can be represented by a moment tensor. We have succeeded in obtaining general expressions for internal deformation due to a moment tensor in an elastic/viscoelastic multilayered half-space under gravity. First, starting from Stokes' classical solution, we obtained the expressions for static displacement fields due to a moment tensor in an infinite elastic medium. Then, performing the Hankel transformation of the static solution in Cartesian coordinates, we derived static displacement potentials for a moment tensor in cylindrical coordinates. Second, representing internal deformation fields by the superposition of a particular solution calculated from the displacement potentials and the general solution for an elastic multilayered half-space without sources, and using the generalized propagator matrix method, we obtained exact expressions for internal elastic deformation fields due to a moment tensor. Finally, applying the correspondence principle of linear viscoelasticity to the elastic solution, we obtained general expressions for quasi-static internal deformation fields due to a moment tensor in an elastic/viscoelastic multilayered half-space. The moment tensor can be generally decomposed into the three independent force systems corresponding to isotropic expansion, crack opening and shear faulting, and so the general expressions include internal deformation fields for these force systems as special cases. As numerical examples we computed the quasi-static internal displacement fields associated with dyke intrusion, episodic segmental ridge opening and steady plate divergence in an elastic–viscoelastic two-layered half-space. We also demonstrated the usefulness of the source representation with moment tensor through the numerical simulation of deformation cycles associated with the periodic occurrence of interplate earthquakes in a ridge–transform fault system.

**Key words:** Transient deformation; Elasticity and anelasticity; Mid-ocean ridge processes; Kinematics of crustal and mantle deformation; Mechanics, theory, and modelling.

## 1 INTRODUCTION

Since Steketee (1958a, b) introduced the concept of dislocation into seismology, mathematical expressions for static deformation fields caused by shear faulting in an elastic half-space have been obtained by many investigators (Chinnery 1961, 1963; Maruyama 1964; Press 1965; Savage & Hastie 1966; Mansinha & Smylie 1971; Sato & Matsu'ura 1974; Iwasaki & Sato 1979; Matsu'ura & Tanimoto 1980; Okada 1992). The elastic half-space model is a simple and good approximation to the real Earth for instantaneous coseismic crustal deformation. For long-term crustal deformation, however, the elastic half-space model is no longer good approximation, because we cannot neglect the effects of stress relaxation in the viscoelastic asthenosphere underlying the elastic lithosphere (e.g. Nur & Mavko 1974; Savage & Prescott 1978; Thatcher & Rundle 1979, 1984; Matsu'ura & Iwasaki 1983; Matsu'ura & Sato 1989; Sato & Matsu'ura 1992, 1993; Hashimoto & Matsu'ura 2000; Hashimoto *et al.* 2004). In general, the viscoelastic solutions of quasi-static problems can be obtained from the associated elastic solutions by applying the correspondence principle of linear viscoelasticity (Lee 1955; Radok 1957), and so we need to obtain elastic solutions for layered Earth models first.

For layered half-space models the mathematical expressions of surface deformation due to shear faulting have been derived with two similar but different approaches. On the basis of general source representation (Ben-Menahem & Singh 1968a, b), Singh (1970), Jovanovich *et al.* (1974a, b) and Rundle (1980) have obtained the elastic solutions with the up–going algorithm of the Thomson–Haskell propagator matrix method (Thomson 1950; Haskell 1953). Applying the correspondence principle of linear viscoelasticity to these elastic solutions, Rundle (1978, 1982a) has obtained the quasi-static solutions for an elastic–viscoelastic layered half-space. On the other hand, Sato (1971), Sato &

Matsu'ura (1973) and Matsu'ura & Sato (1975) have obtained the elastic solutions with the down-going algorithm of the propagator matrix method. Applying the correspondence principle to these elastic solutions, Matsu'ura *et al.* (1981), Iwasaki & Matsu'ura (1981) and Matsu'ura & Sato (1989) have obtained the quasi-static solutions for an elastic-viscoelastic layered half-space.

The solutions derived with the up-going algorithm and those with the down-going algorithm are outwardly similar, but they are essentially different in a computational point of view. Fukahata & Matsu'ura (2005) have revealed that the solutions derived with the up-going algorithm become unstable above the source depth, and those with the down-going algorithm become unstable below the source depth. For example, Roth (1990) and Ma & Kusznir (1992) have obtained the expressions for internal elastic deformation fields by extending the formulation of Singh (1970). Their expressions become numerically unstable above the source depth. On the other hand, Matsu'ura & Sato (1997) have obtained the expressions for internal viscoelastic deformation fields by extending the formulation of Matsu'ura *et al.* (1981). Their expressions become numerically unstable below the source depth. Then, one way to avoid the numerical instability is to use the down-going algorithm above the source depth and the up-going algorithm below the source depth. Pan (1997) and Wang (1999) took this way to obtain numerically stable expressions for internal elastic deformation fields. Another way is to use a static (zero-frequency) version of the generalized reflection and transmission coefficient matrix method (Kennett 1983). Xie & Yao (1989) took this way to obtain numerically stable expressions for elastic internal deformation fields. Recently, by introducing the generalized propagator matrix that unifies the up-going and down-going algorithms, Fukahata & Matsu'ura (2005) have obtained numerically stable expressions for elastic internal deformation fields. Applying the correspondence principle of linear viscoelasticity to this elastic solution, Fukahata & Matsu'ura (2006) have obtained general expressions for internal deformation fields due to shear faulting in an elastic/viscoelastic multilayered half-space under gravity.

As to isotropic expansion and crack opening in a layered half-space, on the other hand, we have not yet obtained the complete expressions for internal deformation fields. For example, Rundle (1978, 1982b) and Fernández & Rundle (1994) have obtained the expression for elastic surface deformation due to isotropic expansion. Folch *et al.* (2000) and Fernández *et al.* (2001) have obtained expressions for viscoelastic surface deformation due to isotropic expansion. Roth (1993) has derived the expressions for internal elastic deformation fields due to crack opening by extending his formulation of shear faulting (Roth 1990). Hofton *et al.* (1995) have obtained viscoelastic surface deformation due to crack opening. In the derivation of these expressions, however, only the up-going algorithm of the propagator matrix method is used, and so they are numerically unstable above the source depth. On the other hand, He *et al.* (2003a) have obtained the expressions for elastic internal deformation fields due to isotropic expansion and crack opening by extending the formulation of Xie & Yao (1989) for shear faulting, based on the generalized reflection and transmission coefficient matrix method.

In the framework of elasticity theory any indigenous source can be represented by a moment tensor (Backus & Mulcahy 1976a, b). The moment tensor, which is a second-order symmetric tensor with the diagonal elements of force dipoles and the off-diagonal elements of force couples, can be decomposed into three independent force systems corresponding to isotropic expansion, crack opening and shear faulting. By using the generalized reflection and transmission coefficient matrix method, He *et al.* (2003b) have formulated surface deformation due to a moment tensor in an elastic layered half-space. In the present study, extending the formulation of Fukahata & Matsu'ura (2005, 2006) for shear faulting, we obtain general expressions for internal displacement fields due to a moment tensor in an elastic/viscoelastic multilayered half-space. In Section 2, we derive the expressions of static displacement potentials in cylindrical coordinates by performing the Hankel transformation of Stokes' classical solution in Cartesian coordinates. In Section 3, we obtain the expressions for internal displacement fields due to a moment tensor in an elastic multilayered half-space. In Section 4, applying the correspondence principle of linear viscoelasticity to the elastic solution, we obtain the expressions for internal displacement fields due to a moment tensor in an elastic/viscoelastic multilayered half-space. In Section 5, as numerical examples, we show the quasi-static internal displacement fields associated with dyke intrusion, episodic segmental ridge opening and steady plate divergence in the case of an elastic-viscoelastic two-layered half-space. We also show the deformation cycle associated with the periodic occurrence of interplate earthquakes in a ridge-transform fault system.

## 2 STATIC DEFORMATION CAUSED BY A MOMENT TENSOR

### 2.1 Displacement potentials in cylindrical coordinates

We consider an infinite elastic medium with the following constitutive equation:

$$\sigma_{kk} = 3K \varepsilon_{kk}, \quad \sigma'_{ij} = 2\mu \varepsilon'_{ij} \tag{1}$$

with

$$\sigma'_{ij} = \sigma_{ij} - \frac{1}{3} \sigma_{kk} \delta_{ij}, \quad \varepsilon'_{ij} = \varepsilon_{ij} - \frac{1}{3} \varepsilon_{kk} \delta_{ij}, \tag{2}$$

where  $\sigma_{ij}$  and  $\varepsilon_{ij}$  denote stress and strain tensors, respectively, and  $K$  and  $\mu$  are the bulk modulus and rigidity of the medium, respectively. Infinitesimal deformation of the elastic medium is governed by well-known Navier's equation:

$$\rho \frac{\partial^2 u_i}{\partial t^2} = \left( K + \frac{1}{3} \mu \right) \frac{\partial}{\partial x_i} \left( \frac{\partial u_j}{\partial x_j} \right) + \mu \frac{\partial}{\partial x_j} \left( \frac{\partial u_i}{\partial x_j} \right) + f_i, \tag{3}$$

where  $\rho$  is density, and  $u_i$  ( $i = 1, 2, 3$ ) and  $f_i$  ( $i = 1, 2, 3$ ) are displacement and body force vectors, respectively. Stokes (1849) has obtained a particular solution (Green's tensor) of Navier's equation for a unit impulsive point force  $f_i = \delta_{ip} \delta(\mathbf{x} - \boldsymbol{\xi}) \delta(t - \tau)$  in Cartesian coordinates

$(x_1, x_2, x_3)$  as

$$G_{ip}(\mathbf{x}, t; \boldsymbol{\xi}, 0) = \frac{3\zeta_i\zeta_p - \delta_{ip}}{4\pi\rho R^3} \int_{R/\alpha}^{R/\beta} s\delta(t-s)ds + \frac{\zeta_i\zeta_p}{4\pi\rho\alpha^2 R} \delta(t - R/\alpha) - \frac{\zeta_i\zeta_p - \delta_{ip}}{4\pi\rho\beta^2 R} \delta(t - R/\beta) \tag{4}$$

with

$$R = \sqrt{(x_1 - \xi_1)^2 + (x_2 - \xi_2)^2 + (x_3 - \xi_3)^2}, \tag{5}$$

$$\zeta_i = \frac{x_i - \xi_i}{R} = \frac{\partial R}{\partial x_i}. \tag{6}$$

Here,  $\alpha$  and  $\beta$  are the  $P$ - and  $S$ -wave velocities of the medium, and  $\delta_{ij}$  is the Kronecker delta.

The dynamic displacement field  $u_i^d(\mathbf{x}, t)$  caused by the moment tensor  $M_{pq}(\tau)$  acting for  $\tau \geq 0$  at a point  $\boldsymbol{\xi} = \mathbf{0}$  is written in the form of convolution integral:

$$u_i^d(\mathbf{x}, t) = \int_0^t G_{ip,q}(\mathbf{x}, t - \tau; \mathbf{0}, 0) M_{pq}(\tau) d\tau, \tag{7}$$

where  $G_{ip,q}$  represents the partial derivatives of Green's tensor  $G_{ip}$  with respect to the source coordinate  $\xi_q$ . The exact expression of  $u_i^d(\mathbf{x}, t)$ , which can be obtained by substituting eq. (4) into eq. (7), is given in Aki & Richards (1980). On the assumption that  $M_{pq}(t)$  becomes a constant  $M_{pq}$  at  $t \rightarrow \infty$ , taking the limit of  $t \rightarrow \infty$  for the exact dynamic solution, we can directly obtain the corresponding static solution  $u_i^s(\mathbf{x})$  as

$$u_i^s(\mathbf{x}) = \frac{1}{8\pi\mu R^2} [\gamma(3\zeta_i\zeta_p\zeta_q - \zeta_i\delta_{pq} - \zeta_p\delta_{qi} - \zeta_q\delta_{ip}) + 2\zeta_q\delta_{ip}] M_{pq} \tag{8}$$

with

$$\gamma = (3K + \mu)/(3K + 4\mu). \tag{9}$$

By using the relations in eq. (6), the above solution can be rewritten in vector form:

$$\mathbf{u}^s(\mathbf{x}) = \frac{1}{8\pi\mu} [(\gamma - 1)\nabla(\nabla \cdot \mathbf{s}) + \nabla \times \nabla \times \mathbf{s}] \tag{10}$$

with

$$\mathbf{s} = \mathbf{M}\nabla R. \tag{11}$$

Now we perform the transformation of variables from Cartesian coordinates  $(x_1, x_2, x_3)$  to cylindrical coordinates  $(r, \varphi, z)$ :

$$x_1 = r \cos \varphi, \quad x_2 = r \sin \varphi, \quad x_3 = z. \tag{12}$$

Then, the elements of moment tensor  $\mathbf{M}$  in cylindrical coordinates are related with those in Cartesian coordinates as

$$\begin{pmatrix} M_{rr} & M_{r\varphi} & M_{rz} \\ M_{\varphi r} & M_{\varphi\varphi} & M_{\varphi z} \\ M_{zr} & M_{z\varphi} & M_{zz} \end{pmatrix} = \begin{pmatrix} \cos \varphi & \sin \varphi & 0 \\ -\sin \varphi & \cos \varphi & 0 \\ 0 & 0 & 1 \end{pmatrix} \begin{pmatrix} M_{11} & M_{12} & M_{13} \\ M_{21} & M_{22} & M_{23} \\ M_{31} & M_{32} & M_{33} \end{pmatrix} \begin{pmatrix} \cos \varphi & -\sin \varphi & 0 \\ \sin \varphi & \cos \varphi & 0 \\ 0 & 0 & 1 \end{pmatrix} \tag{13}$$

and the distance  $R$  in eq. (5) is expressed as

$$R = \sqrt{r^2 + z^2}. \tag{14}$$

In static problems, as Takeuchi (1959) has shown, a proper representation of solution vectors  $\mathbf{u}^s$  in terms of displacement potentials,  $\Phi_1^s$ ,  $\Phi_2^s$  and  $\Psi^s$ , is given by

$$\mathbf{u}^s = \nabla\Phi_1^s - \gamma z\nabla\Phi_2^s + (2 - \gamma) \begin{pmatrix} 0 \\ 0 \\ \Phi_2^s \end{pmatrix} + \nabla \times \begin{pmatrix} 0 \\ 0 \\ \Psi^s \end{pmatrix}. \tag{15}$$

Comparing the above general representation with the specific expression for a moment tensor in eq. (10), we obtain a set of equations to be solved for the displacement potentials:

$$\frac{\partial}{\partial z} (\Phi_1^s - \gamma z\Phi_2^s) + 2\Phi_2^s = \frac{1}{8\pi\mu} \left( \gamma \frac{\partial}{\partial z} \nabla \cdot \mathbf{s} - \nabla^2 \mathbf{s}_z \right) \tag{16}$$

$$\left( \frac{\partial^2}{\partial z^2} - \nabla^2 \right) \Psi^s = \frac{1}{8\pi\mu} (\nabla \times \nabla \times \nabla \times \mathbf{s})_z \tag{17}$$

$$2 \left( \frac{\partial^2}{\partial z^2} - \nabla^2 \right) \Phi_2^s = \frac{1}{8\pi\mu} (\nabla \times \nabla \times \nabla \times \nabla \times \mathbf{s})_z, \tag{18}$$

where the subscript  $z$  denotes the  $z$ -component of the corresponding vector. From eqs (16)–(18) and eq. (11), using a basic formula of Hankel transform

$$\frac{1}{R} = \frac{1}{\sqrt{r^2 + z^2}} = \int_0^\infty e^{-\xi|z|} J_0(\xi r) d\xi, \tag{19}$$

we can obtain explicit expressions for the displacement potentials in cylindrical coordinates in the form of semi-infinite integral with respect to wave number  $\xi$ :

$$\Phi_1^s(r, \varphi, z) = \frac{1}{4\pi\mu} \int_0^\infty \left\{ -\frac{1}{4}[(2-\gamma)(M_{rr} + M_{\varphi\varphi}) - 2\gamma M_{zz}]J_0(\xi r) + \operatorname{sgn}(z)M_{rz}J_1(\xi r) + \frac{2-\gamma}{4}(M_{rr} - M_{zz})J_2(\xi r) \right\} e^{-\xi|z|} d\xi \quad (20)$$

$$\Phi_2^s(r, \varphi, z) = \frac{1}{4\pi\mu} \int_0^\infty \left\{ -\operatorname{sgn}(z)\frac{1}{4}[(M_{rr} + M_{\varphi\varphi}) - 2M_{zz}]J_0(\xi r) + M_{rz}J_1(\xi r) + \operatorname{sgn}(z)\frac{1}{4}(M_{rr} - M_{\varphi\varphi})J_2(\xi r) \right\} \xi e^{-\xi|z|} d\xi \quad (21)$$

$$\Psi^s(r, \varphi, z) = -\frac{1}{4\pi\mu} \int_0^\infty [\operatorname{sgn}(z)M_{\varphi z}J_1(\xi r) + M_{r\varphi}J_2(\xi r)]e^{-\xi|z|} d\xi, \quad (22)$$

where  $J_n(\xi r)$  is the  $n$ th order Bessel function and  $\operatorname{sgn}(z)$  denotes the sign function that takes the value of 1 for  $z > 0$  and  $-1$  for  $z < 0$ . It should be noted that all of these potentials satisfy the Laplace equation except for  $z = 0$ .

We rewrite eqs (20)–(22) in the following more concise form:

$$\begin{cases} \Phi_1^s(r, \varphi, z) = \frac{1}{4\pi} \int_0^\infty \chi_1^s(z; \xi) \mathbf{j}(r, \varphi; \xi) d\xi \\ \Phi_2^s(r, \varphi, z) = \frac{1}{4\pi} \int_0^\infty \chi_2^s(z; \xi) \mathbf{j}(r, \varphi; \xi) \xi d\xi \\ \Psi^s(r, \varphi, z) = \frac{1}{4\pi} \int_0^\infty \chi^s(z; \xi) \mathbf{j}'(r, \varphi; \xi) d\xi \end{cases} \quad (23)$$

Here,  $\chi_1^s$ ,  $\chi_2^s$  and  $\chi^s$  are the  $z$ -dependent coefficient vectors defined by

$$\begin{cases} \chi_1^s(z; \xi) = [1 - 4\gamma \quad 2 + \gamma \quad -\operatorname{sgn}(z) \quad 2 - \gamma]e^{-\xi|z|} \\ \chi_2^s(z; \xi) = [0 \quad 3\operatorname{sgn}(z) \quad -1 \quad \operatorname{sgn}(z)]e^{-\xi|z|} \\ \chi^s(z; \xi) = [\operatorname{sgn}(z) \quad -1]e^{-\xi|z|} \end{cases} \quad (24)$$

and  $\mathbf{j}$  and  $\mathbf{j}'$  are the  $r$ - and  $\varphi$ -dependent source vectors defined by

$$\mathbf{j}(r, \varphi; \xi) = \begin{bmatrix} m_1 J_0(\xi r) \\ m_2 J_0(\xi r) \\ m_3 \cos \varphi J_1(\xi r) + m_4 \sin \varphi J_1(\xi r) \\ m_5 \cos 2\varphi J_2(\xi r) + m_6 \sin 2\varphi J_2(\xi r) \end{bmatrix} \quad (25)$$

$$\mathbf{j}'(r, \varphi; \xi) = \begin{bmatrix} -m_3 \sin \varphi J_1(\xi r) + m_4 \cos \varphi J_1(\xi r) \\ -2m_5 \sin 2\varphi J_2(\xi r) + 2m_6 \cos 2\varphi J_2(\xi r) \end{bmatrix} \quad (26)$$

with

$$m_1 = \frac{M_{11} + M_{22} + M_{33}}{9K}, \quad m_2 = \frac{-M_{11} - M_{22} + 2M_{33}}{12\mu}, \quad m_3 = -\frac{M_{13}}{\mu}, \quad m_4 = -\frac{M_{23}}{\mu}, \quad m_5 = \frac{M_{11} - M_{22}}{4\mu}, \quad m_6 = \frac{M_{12}}{2\mu}. \quad (27)$$

Each component of the source vectors  $\mathbf{j}$  and  $\mathbf{j}'$  represents a horizontal mode solution corresponding to some force system composed of the elements of moment tensor  $M_{pq}$ . Substituting the expressions of displacement potentials in eq. (23) into eq. (15), we can obtain the explicit expressions for displacement fields due to a moment tensor in cylindrical coordinates.

### 2.2 Specific representation of source vectors

There are many ways to decompose a moment tensor into several independent force systems. It is natural to decompose a moment tensor into two force systems corresponding to isotropic expansion and displacement discontinuity across an internal surface. The displacement discontinuity vector can be decomposed into the normal and tangential components, which correspond to crack opening and shear faulting, respectively. Therefore, we can decompose a moment tensor into three independent force systems corresponding to isotropic expansion, crack

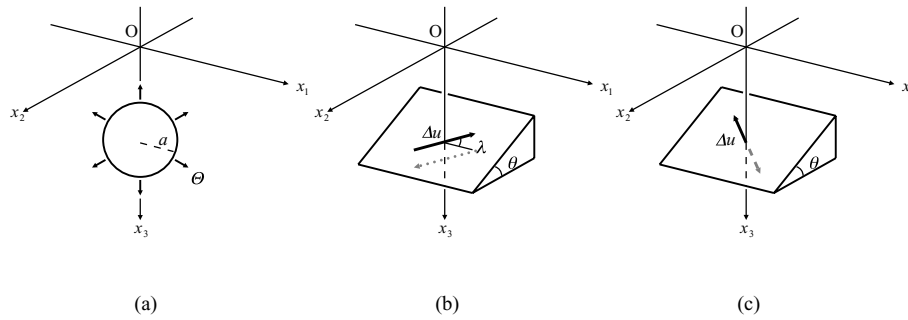


Figure 1. Three basic physical processes represented by a moment tensor: (a) isotropic expansion, (b) shear faulting, and (c) crack opening.

opening and shear faulting. This decomposition is natural and always possible by solving the eigenvalue problems of moment tensor. In this section we show the explicit expressions of the source vectors  $\mathbf{j}$  and  $\mathbf{j}'$  for isotropic expansion, crack opening and shear faulting.

2.2.1 Isotropic expansion

A fractional volume change  $\Theta = \Delta V/V$  in an infinitesimal sphere with a radius  $a$  (Fig. 1a) can be expressed in terms of a moment tensor as

$$M_{pq} = \frac{4\pi a^3}{3} K \Theta \delta_{pq}. \tag{28}$$

Substituting eq. (28) into eqs (25) and (26) with eq. (27), we obtain the expressions of  $\mathbf{j}$  and  $\mathbf{j}'$  for isotropic expansion as

$$\mathbf{j}(r, \varphi; \xi) = \frac{4}{9} \pi a^3 \Theta \begin{bmatrix} J_0(\xi r) \\ 0 \\ 0 \\ 0 \end{bmatrix}, \quad \mathbf{j}'(r, \varphi; \xi) = \begin{pmatrix} 0 \\ 0 \\ 0 \end{pmatrix}. \tag{29}$$

2.2.2 Shear faulting and crack opening

A displacement discontinuity  $\Delta \mathbf{u}$  with a unit direction vector  $\boldsymbol{\nu} = (\nu_1, \nu_2, \nu_3)$  on an infinitesimal fault plane  $d\Sigma$  with a unit normal vector  $\mathbf{n} = (n_1, n_2, n_3)$  can be expressed in terms of a moment tensor as

$$M_{pq} = \Delta u d\Sigma \left[ K n_k \nu_k \delta_{pq} + \mu \left( n_p \nu_q + n_q \nu_p - \frac{2}{3} n_k \nu_k \delta_{pq} \right) \right]. \tag{30}$$

The above expression includes both cases of shear faulting ( $\mathbf{n} \cdot \boldsymbol{\nu} = 0$ ) and crack opening ( $\mathbf{n} \cdot \boldsymbol{\nu} = 1$ ). We first consider the case of shear faulting on an inclined plane with its strike parallel to the  $x_1$ -axis, a dip angle  $\theta$ , and a slip angle  $\lambda$  (Fig. 1b). In this case the components of the direction vector  $\boldsymbol{\nu}$  and the normal vector  $\mathbf{n}$  are given as

$$\mathbf{n} = (0, \sin\theta, -\cos\theta), \quad \boldsymbol{\nu} = (\cos\lambda, -\sin\lambda \cos\theta, -\sin\lambda \sin\theta). \tag{31}$$

Substituting eqs (30) and (31) into eqs (25) and (26) with eq. (27), we obtain the expressions of  $\mathbf{j}$  and  $\mathbf{j}'$  for shear faulting as

$$\mathbf{j}(r, \varphi; \xi) = \Delta u d\Sigma \begin{bmatrix} 0 \\ \frac{1}{4} \sin 2\theta \sin \lambda J_0(\xi r) \\ (\cos \lambda \cos \theta \cos \varphi - \sin \lambda \cos 2\theta \sin \varphi) J_1(\xi r) \\ \frac{1}{4} (\sin \lambda \sin 2\theta \cos 2\varphi + 2 \cos \lambda \sin \theta \sin 2\varphi) J_2(\xi r) \end{bmatrix} \tag{32}$$

$$\mathbf{j}'(r, \varphi; \xi) = \Delta u d\Sigma \begin{bmatrix} -(\cos \lambda \cos \theta \sin \varphi + \sin \lambda \cos 2\theta \cos \varphi) J_1(\xi r) \\ -\frac{1}{2} (\sin \lambda \sin 2\theta \sin 2\varphi - 2 \cos \lambda \sin \theta \cos 2\varphi) J_2(\xi r) \end{bmatrix}. \tag{33}$$

Note that the first component of the source vector  $\mathbf{j}$  is always zero for shear faulting. Sato (1971) has obtained the representation of source vectors equivalent to those in eqs (32) and (33).

In the case of crack opening on a plane with its strike parallel to the  $x_1$ -axis and a dip angle  $\theta$  (Fig. 1c), since the direction vector  $\boldsymbol{\nu}$  is parallel to the normal vector  $\mathbf{n}$ , we have

$$\mathbf{n} = \boldsymbol{\nu} = (0, \sin\theta, -\cos\theta). \tag{34}$$

In the same way as in the case of shear faulting, substituting eqs (30) and (34) into eqs (25) and (26) with eq. (27), we obtain the expressions of  $\mathbf{j}$  and  $\mathbf{j}'$  for crack opening as

$$\mathbf{j}(r, \varphi; \xi) = \Delta u d \Sigma \begin{bmatrix} \frac{1}{3} J_0(\xi r) \\ \frac{1}{6} (3 \cos^2 \theta - 1) J_0(\xi r) \\ \sin 2\theta \sin \varphi J_1(\xi r) \\ -\frac{1}{2} \sin^2 \theta \cos 2\varphi J_2(\xi r) \end{bmatrix}, \quad \mathbf{j}'(r, \varphi; \xi) = \Delta u d \Sigma \begin{bmatrix} \sin 2\theta \cos \varphi J_1(\xi r) \\ \sin^2 \theta \sin 2\varphi J_2(\xi r) \end{bmatrix}. \quad (35)$$

### 3 ELASTIC SOLUTION FOR A LAYERED HALF-SPACE

We consider the elastic medium composed of  $n - 1$  parallel layers overlying a half-space as shown in Fig. 2. Here, every layer and interface is numbered in ascending order from the free surface, and the positive  $z$ -axis is taken as directed into the medium. The depth of the  $j$ th interface is denoted by  $H_j$ , and the thickness of the  $j$ th layer by  $h_j$ . We use bulk modulus  $K_j$  and rigidity  $\mu_j$ , or  $\gamma_j = (3K_j + \mu_j)/(3K_j + 4\mu_j)$  and  $\mu_j$ , to represent the elastic property of the  $j$ th layer. A point moment tensor  $\mathbf{M}H(t)$  is located at  $(0, 0, d)$  in the  $m$ th layer. Here, we use the Heaviside step function  $H(t)$  to represent an instantaneous source time process at  $t = 0$ . Then, in a layer with the source ( $j = m$ ), the elastic displacement field  $\mathbf{u}^E(r, \varphi, z, t; j)$  can be represented by the sum of a particular solution  $\mathbf{u}^s(r, \varphi, z - d, t; j)$  for an infinite medium with the source, which is obtained by substituting the displacement potentials in eq. (23) into eq. (15), and the general solution  $\mathbf{u}^g(r, \varphi, z, t; j)$  for the layer without sources, which is obtained by superposing mode solutions of the Laplace equation. In a layer without sources ( $j \neq m$ ), on the other hand, the elastic displacement field  $\mathbf{u}^E$  is given by the general solution  $\mathbf{u}^g$ . Thus we can generally represent the elastic displacement field as

$$\mathbf{u}^E(r, \varphi, z, t; j) = \mathbf{u}^g(r, \varphi, z, t; j) + \delta_{jm} \mathbf{u}^s(r, \varphi, z - d, t; m). \quad (36)$$

#### 3.1 Representation of internal deformation fields

We represent the general solution  $\mathbf{u}^g$  of the  $j$ th layer ( $H_{j-1} \leq z \leq H_j$ ) by using displacement potentials,  $\Phi_{1j}^g$ ,  $\Phi_{2j}^g$  and  $\Psi_j^g$ , in the same form as eq. (15):

$$\mathbf{u}^g(r, \varphi, z; j) = \nabla \Phi_{1j}^g - \gamma_j (z - H_{j-1}) \nabla \Phi_{2j}^g + (2 - \gamma_j) \begin{pmatrix} 0 \\ 0 \\ \Phi_{2j}^g \end{pmatrix} + \nabla \times \begin{pmatrix} 0 \\ 0 \\ \Psi_j^g \end{pmatrix}. \quad (37)$$

General expressions for the displacement potentials are given by the superposition of all the mode solutions of the Laplace equation. From among all the mode solutions we choose some specific ones corresponding to the horizontal modes in the particular solution to satisfy boundary

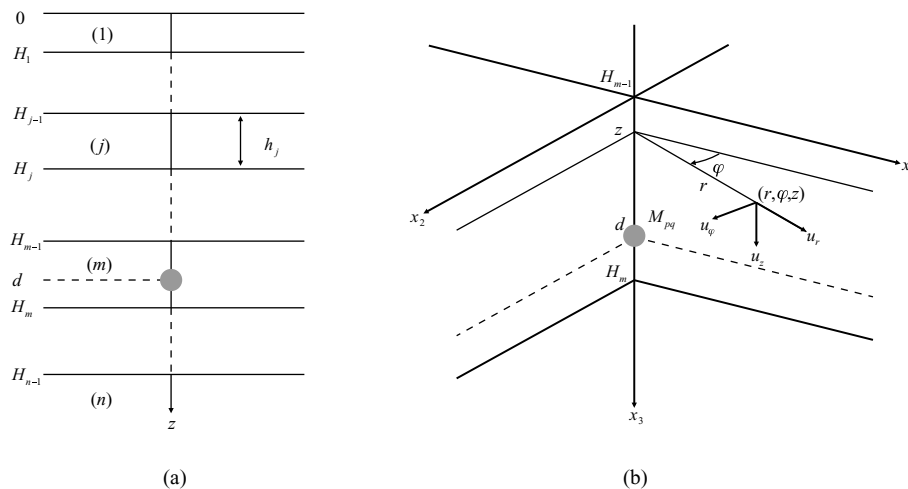


**Figure 2.** The coordinate system, source geometry, and a layered structure model. Every layer and interface is numbered in ascending order from the free surface. The direction of the  $x_3$ -axis in Cartesian coordinates or the  $z$ -axis in cylindrical coordinates is taken to be vertically downward. The depth of the  $j$ th interface is denoted by  $H_j$ , and the thickness of the  $j$ th layer by  $h_j = H_j - H_{j-1}$ . The source is located at  $(0, 0, d)$  on the  $z$ -axis.

conditions. Thus, by using the same source vectors  $\mathbf{j}$  and  $\mathbf{j}'$  in eqs (25) and (26), we may write the displacement potentials of  $\mathbf{u}^g$  in the following integral form:

$$\begin{cases} \Phi_{1j}^g(r, \varphi, z) = \frac{1}{4\pi} \int_0^\infty \chi_{1j}^g(z; \xi) \mathbf{j}(r, \varphi; \xi) d\xi \\ \Phi_{2j}^g(r, \varphi, z) = \frac{1}{4\pi} \int_0^\infty \chi_{2j}^g(z; \xi) \mathbf{j}(r, \varphi; \xi) \xi d\xi \\ \Psi_j^g(r, \varphi, z) = \frac{1}{4\pi} \int_0^\infty \chi_j^g(z; \xi) \mathbf{j}'(r, \varphi; \xi) d\xi \end{cases} \quad (38)$$

with the  $z$ -dependent coefficient vectors  $\chi_{1j}^g$ ,  $\chi_{2j}^g$  and  $\chi_j^g$  defined by

$$\begin{cases} \chi_{1j}^g(z; \xi) = (1 - \delta_{jn}) \left( A_{1j}^+ \ A_{2j}^+ \ A_{3j}^+ \ A_{4j}^+ \right) e^{\xi(z-H_{j-1})} + \left( A_{1j}^- \ A_{2j}^- \ A_{3j}^- \ A_{4j}^- \right) e^{-\xi(z-H_{j-1})} \\ \chi_{2j}^g(z; \xi) = (1 - \delta_{jn}) \left( B_{1j}^+ \ B_{2j}^+ \ B_{3j}^+ \ B_{4j}^+ \right) e^{\xi(z-H_{j-1})} + \left( B_{1j}^- \ B_{2j}^- \ B_{3j}^- \ B_{4j}^- \right) e^{-\xi(z-H_{j-1})} \\ \chi_j^g(z; \xi) = (1 - \delta_{jn}) \left( C_{1j}^+ \ C_{2j}^+ \right) e^{\xi(z-H_{j-1})} + \left( C_{1j}^- \ C_{2j}^- \right) e^{-\xi(z-H_{j-1})} \end{cases} \quad (39)$$

Here,  $A_{kj}^\pm$  ( $k = 1, 2, 3, 4$ ),  $B_{kj}^\pm$  ( $k = 1, 2, 3, 4$ ) and  $C_{kj}^\pm$  ( $k = 1, 2$ ) are the  $\xi$ -dependent potential coefficients to be determined from boundary conditions. It should be noted that the terms exponentially increasing with depth  $z$  must be removed from eq. (39) for the substratum ( $j = n$ ), because every displacement and stress components do not diverge at  $z \rightarrow \infty$  from causality.

Substituting eq. (23) and (38) into eq. (15) and (37), respectively, we obtain expressions for  $u_{r(\varphi,z)}^s(r, \varphi, z, t; m)$  and  $u_{r(\varphi,z)}^g(r, \varphi, z, t; j)$  in the same integral form. We combine them by eq. (36) to obtain the formal expressions for elastic displacement fields  $u_{r(\varphi,z)}^E(r, \varphi, z, t; j)$  due to a moment tensor  $\mathbf{MH}(t)$  at a point  $(0, 0, d)$  in the  $m$ th layer:

$$\begin{cases} u_r^E(r, \varphi, z, t; j) = \frac{H(t)}{4\pi} \int_0^\infty \left[ \mathbf{y}_1^E(z; \xi; j) \frac{\partial}{\partial r} \mathbf{j}(r, \varphi; \xi) + \mathbf{y}'_1^E(z; \xi; j) \frac{1}{r} \frac{\partial}{\partial \varphi} \mathbf{j}'(r, \varphi; \xi) \right] d\xi \\ u_\varphi^E(r, \varphi, z, t; j) = \frac{H(t)}{4\pi} \int_0^\infty \left[ \mathbf{y}_1^E(z; \xi; j) \frac{1}{r} \frac{\partial}{\partial \varphi} \mathbf{j}(r, \varphi; \xi) - \mathbf{y}'_1^E(z; \xi; j) \frac{\partial}{\partial r} \mathbf{j}'(r, \varphi; \xi) \right] d\xi \\ u_z^E(r, \varphi, z, t; j) = \frac{H(t)}{4\pi} \int_0^\infty \mathbf{y}_2^E(z; \xi; j) \mathbf{j}(r, \varphi; \xi) \xi d\xi \end{cases} \quad (40)$$

The corresponding expressions for stress components  $\sigma_{zr(\varphi,z)}^E(r, \varphi, z, t; j)$  are calculated from the displacement potentials in eqs (23) and (38) by the definition of stress components in cylindrical coordinates as

$$\begin{cases} \sigma_{zr}^E(r, \varphi, z, t; j) = \frac{\mu_j H(t)}{4\pi} \int_0^\infty \left[ 2\mathbf{y}_3^E(z; \xi; j) \frac{\partial}{\partial r} \mathbf{j}(r, \varphi; \xi) + \mathbf{y}'_2^E(z; \xi; j) \frac{1}{r} \frac{\partial}{\partial \varphi} \mathbf{j}'(r, \varphi; \xi) \right] \xi d\xi \\ \sigma_{z\varphi}^E(r, \varphi, z, t; j) = \frac{\mu_j H(t)}{4\pi} \int_0^\infty \left[ 2\mathbf{y}_3^E(z; \xi; j) \frac{1}{r} \frac{\partial}{\partial \varphi} \mathbf{j}(r, \varphi; \xi) - \mathbf{y}'_2^E(z; \xi; j) \frac{\partial}{\partial r} \mathbf{j}'(r, \varphi; \xi) \right] \xi d\xi \\ \sigma_{zz}^E(r, \varphi, z, t; j) = \frac{\mu_j H(t)}{4\pi} \int_0^\infty 2\mathbf{y}_4^E(z; \xi; j) \mathbf{j}(r, \varphi; \xi) \xi^2 d\xi \end{cases} \quad (41)$$

Here, for the source vectors  $\mathbf{j}(r, \varphi; \xi)$  and  $\mathbf{j}'(r, \varphi; \xi)$ , we have already obtained the definite expressions in eqs (25) and (26). Thus, our problem is to determine the  $z$ -dependent deformation vectors,  $\mathbf{y}_k^E$  ( $k = 1, 2, 3, 4$ ) and  $\mathbf{y}'_k^E$  ( $k = 1, 2$ ) from boundary conditions at the Earth's surface and layer interfaces.

### 3.2 Deformation matrices and boundary conditions

We define the  $4 \times 4$  and  $2 \times 2$  deformation matrices  $\mathbf{Y}^E$  and  $\mathbf{Y}'^E$  composed of the deformation vectors  $\mathbf{y}_k^E$  ( $k = 1, 2, 3, 4$ ) and  $\mathbf{y}'_k^E$  ( $k = 1, 2$ ), respectively, as

$$\mathbf{Y}^E(z; j) = \begin{bmatrix} \mathbf{y}_1^E(z; j) \\ \mathbf{y}_2^E(z; j) \\ \mathbf{y}_3^E(z; j) \\ \mathbf{y}_4^E(z; j) \end{bmatrix}, \quad \mathbf{Y}'^E(z; j) = \begin{bmatrix} \mathbf{y}'_1^E(z; j) \\ \mathbf{y}'_2^E(z; j) \end{bmatrix}. \quad (42)$$

Hereafter we omit the  $\xi$ - and  $t$ -dependence in notation for simplicity. The formal expressions of the deformation matrices, which are composed of the deformation matrices for the particular solution,  $\mathbf{Y}^s$  and  $\mathbf{Y}'^s$ , and those for the general solution,  $\mathbf{Y}^g$  and  $\mathbf{Y}'^g$ , are given as follows:

$$\begin{cases} \mathbf{Y}^E(z; j) = \mathbf{Y}^g(z; j) + \delta_{jm} \exp(-|z-d|\xi) \mathbf{Y}^s(z-d; m) \\ \mathbf{Y}'^E(z; j) = \mathbf{Y}'^g(z; j) + \delta_{jm} \exp(-|z-d|\xi) \mathbf{Y}'^s(z-d; m) \end{cases} \quad (43)$$

where

$$\mathbf{Y}^s(z; m) = \begin{bmatrix} 1 - 4\gamma_m & 2 + \gamma_m(1 - 3|z|\xi) & -\text{sgn}(z) + \gamma_m z \xi & 2 - \gamma_m(1 + |z|\xi) \\ \text{sgn}(z)(4\gamma_m - 1) & 4\text{sgn}(z)(1 - \gamma_m) + 3\gamma_m z \xi & -1 + \gamma_m(1 - |z|\xi) & \gamma_m z \xi \\ \text{sgn}(z)(4\gamma_m - 1) & \text{sgn}(z)(1 - 4\gamma_m) + 3\gamma_m z \xi & \gamma_m(1 - |z|\xi) & -\text{sgn}(z) + \gamma_m z \xi \\ 1 - 4\gamma_m & -1 + \gamma_m(1 - 3|z|\xi) & \gamma_m z \xi & 1 - \gamma_m(1 + |z|\xi) \end{bmatrix} \quad (44)$$

$$\mathbf{Y}^s(z; m) = \begin{bmatrix} \text{sgn}(z) & -1 \\ -1 & \text{sgn}(z) \end{bmatrix}$$

and

$$\mathbf{Y}^g(z; j) = \mathbf{E}_j(z - H_{j-1})\mathbf{A}_j, \quad \mathbf{Y}'^g(z; j) = \mathbf{E}'_j(z - H_{j-1})\mathbf{A}'_j \quad (45)$$

with

$$\mathbf{A}_{j(\neq n)} = \begin{pmatrix} A_{1j}^+ + A_{1j}^- & A_{2j}^+ + A_{2j}^- & A_{3j}^+ + A_{3j}^- & A_{4j}^+ + A_{4j}^- \\ B_{1j}^+ + B_{1j}^- & B_{2j}^+ + B_{2j}^- & B_{3j}^+ + B_{3j}^- & B_{4j}^+ + B_{4j}^- \\ A_{1j}^+ - A_{1j}^- & A_{2j}^+ - A_{2j}^- & A_{3j}^+ - A_{3j}^- & A_{4j}^+ - A_{4j}^- \\ B_{1j}^+ - B_{1j}^- & B_{2j}^+ - B_{2j}^- & B_{3j}^+ - B_{3j}^- & B_{4j}^+ - B_{4j}^- \end{pmatrix}, \quad \mathbf{A}'_{j(\neq n)} = \begin{pmatrix} C_{1j}^+ + C_{1j}^- & C_{2j}^+ + C_{2j}^- \\ C_{1j}^+ - C_{1j}^- & C_{2j}^+ - C_{2j}^- \end{pmatrix}, \quad (46)$$

$$\mathbf{A}_n = \begin{pmatrix} \mathbf{a}_n \\ \mathbf{b}_n \\ -\mathbf{a}_n \\ -\mathbf{b}_n \end{pmatrix} = \begin{pmatrix} A_{1n}^- & A_{2n}^- & A_{3n}^- & A_{4n}^- \\ B_{1n}^- & B_{2n}^- & B_{3n}^- & B_{4n}^- \\ -A_{1n}^- & -A_{2n}^- & -A_{3n}^- & -A_{4n}^- \\ -B_{1n}^- & -B_{2n}^- & -B_{3n}^- & -B_{4n}^- \end{pmatrix}, \quad \mathbf{A}'_n = \begin{pmatrix} \mathbf{c}_n \\ -\mathbf{c}_n \end{pmatrix} = \begin{pmatrix} C_{1n}^- & C_{2n}^- \\ -C_{1n}^- & -C_{2n}^- \end{pmatrix}. \quad (47)$$

Here,  $\mathbf{E}_j$  and  $\mathbf{E}'_j$  are the purely structure-dependent matrices (independent of source properties), whose explicit expressions are given in Appendix A.

The deformation matrices defined in eq. (43) must satisfy the stress-free condition, including the gravitational effects associated with surface uplift and subsidence (McConnell 1965; Matsu'ura & Sato 1989), at the Earth's surface ( $z = 0$ ):

$$\sigma_{zr(\varphi)}(r, \varphi, 0; 1) = 0, \quad \sigma_{zz}(r, \varphi, 0; 1) - \rho_1 g u_z(r, \varphi, 0; 1) = 0, \quad (48)$$

where  $\rho_1$  is the density of the surface layer, and  $g$  is the acceleration of gravity at the Earth's surface. From eqs (40) and (41) the stress-free condition can be written in terms of the deformation vectors as

$$\mathbf{y}_3^E(0; 1) = 0, \quad \mathbf{y}'^E(0; 1) = 0, \quad 2\mu_1 \xi \mathbf{y}_4^E(0; 1) - \rho_1 g \mathbf{y}_2^E(0; 1) = 0, \quad (49)$$

or in terms of the deformation matrices as

$$\mathbf{Y}^E(0; 1) = \mathbf{G}\mathbf{Y}^0, \quad \mathbf{Y}'^E(0; 1) = \mathbf{Y}'^0 \quad (50)$$

with

$$\mathbf{Y}^0 = \begin{pmatrix} \mathbf{y}_1^0 \\ \mathbf{y}_2^0 \\ \mathbf{0} \\ \mathbf{0} \end{pmatrix}, \quad \mathbf{Y}'^0 = \begin{pmatrix} \mathbf{y}'_1^0 \\ \mathbf{0} \end{pmatrix}. \quad (51)$$

Here,  $\mathbf{G}$  is a purely structure-dependent matrix, whose explicit expression is given in Appendix A. At each layer interface ( $z = H_j$ ) every components of the displacement and stress vectors must satisfy the condition of continuity,

$$\begin{cases} u_{r(\varphi, z)}(r, \varphi, H_j^+; j+1) = u_{r(\varphi, z)}(r, \varphi, H_j^-; j) \\ \sigma_{zr(\varphi, z)}(r, \varphi, H_j^+; j+1) = \sigma_{zr(\varphi, z)}(r, \varphi, H_j^-; j) \end{cases}, \quad (52)$$

which can be written in terms of the deformation matrices as

$$\mathbf{Y}^E(H_j^+; j+1) = \mathbf{D}_j \mathbf{Y}^E(H_j^-; j), \quad \mathbf{Y}'^E(H_j^+; j+1) = \mathbf{D}'_j \mathbf{Y}'^E(H_j^-; j). \quad (53)$$

Here,  $\mathbf{D}_j$  and  $\mathbf{D}'_j$  are purely structure-dependent matrices, whose explicit expressions are given in Appendix A. In the above expressions, we ignored the gravitational effects associated with vertical displacements at the layer interfaces, because the density difference between the upper and lower layers is small in comparison with that at the Earth's surface. If we want to include the gravitational effects at the layer interfaces, the matrices  $\mathbf{D}_j$  and  $\mathbf{D}'_j$  in eq. (53) should be slightly modified in a similar way to the case of the Earth's surface (Iwasaki & Matsu'ura 1982).

In addition, using the down-going expressions of the generalized propagator matrices defined by Fukahata & Matsu'ura (2005),

$$\mathbf{F}_j(z) \equiv \mathbf{E}_j(z)\mathbf{E}_j^{-1}(0), \quad \mathbf{F}'_j(z) \equiv \mathbf{E}'_j(z)\mathbf{E}'_j^{-1}(0) = \mathbf{E}'_j(z), \quad (54)$$

we can relate the deformation matrices at the top ( $z = H_{j-1}^+$ ) and the bottom ( $z = H_j^-$ ) of the  $j$ th layer without sources ( $j \neq m, n$ ) as

$$\mathbf{Y}^E(H_j^-; j \neq m) = \mathbf{F}_j(H_j)\mathbf{Y}^E(H_{j-1}^+; j), \quad \mathbf{Y}'^E(H_j^-; j \neq m) = \mathbf{F}'_j(H_j)\mathbf{Y}'^E(H_{j-1}^+; j). \quad (55)$$

Here,  $\mathbf{F}_j(z)$  and  $\mathbf{F}'_j(z)$  are purely structure-dependent matrices. The explicit expression for  $\mathbf{F}_j(z)$  is given in Appendix A together with  $\mathbf{E}_j(0)$  and its inverse  $\mathbf{E}_j^{-1}(0)$ . For the source layer ( $j = m$ ), taking the direct source effects into account, we obtain the following relations:

$$\begin{cases} \mathbf{Y}^E(H_m^-; m) = \mathbf{F}_m(h_m)\mathbf{Y}^E(H_{m-1}^+; m) - \mathbf{F}_m(H_m - d)\Delta_m \\ \mathbf{Y}'^E(H_m^-; m) = \mathbf{F}'_m(h_m)\mathbf{Y}'^E(H_{m-1}^+; m) - \mathbf{F}'_m(H_m - d)\Delta'_m \end{cases} \quad (56)$$

with

$$\Delta_m = \mathbf{Y}^s(0^-; m) - \mathbf{Y}^s(0^+; m), \quad \Delta'_m = \mathbf{Y}'^s(0^-; m) - \mathbf{Y}'^s(0^+; m). \quad (57)$$

The explicit expressions for  $\Delta_m$  and  $\Delta'_m$  are given by

$$\Delta_m = 2 \begin{pmatrix} 0 & 0 & 1 & 0 \\ 1 - 4\gamma_m & -4 + 4\gamma_m & 0 & 0 \\ 1 - 4\gamma_m & -1 + 4\gamma_m & 0 & 1 \\ 0 & 0 & 0 & 0 \end{pmatrix}, \quad \Delta'_m = -2 \begin{pmatrix} 1 & 0 \\ 0 & 1 \end{pmatrix}. \quad (58)$$

For the substratum ( $j = n$ ), from eqs (43) and (45), we obtain

$$\begin{cases} \mathbf{Y}^E(H_{n-1}^+; n) = \mathbf{E}_n(0)\mathbf{A}_n + \delta_{mn} \exp(-|H_{n-1} - d|\xi)\mathbf{Y}^s(H_{n-1} - d; n) \\ \mathbf{Y}'^E(H_{n-1}^+; n) = \mathbf{A}'_n + \delta_{mn} \exp(-|H_{n-1} - d|\xi)\mathbf{Y}'^s(H_{n-1} - d; n) \end{cases} \quad (59)$$

By using the relations (55), (56) and (59) and the boundary conditions (50) and (53), the deformation matrices can be connected from the top to the bottom of the layered half-space in the down-going way as

$$\mathbf{A}_n = \mathbf{P}\mathbf{Y}^0 - \mathbf{Q}^m, \quad \mathbf{A}'_n = \mathbf{P}'\mathbf{Y}'^0 - \mathbf{Q}'^m \quad (60)$$

with

$$\mathbf{P} = \mathbf{E}_n^{-1}(0) \prod_{j=1}^{n-1} [\mathbf{D}_{n-j}\mathbf{F}_{n-j}(h_{n-j})]\mathbf{G}, \quad \mathbf{P}' = \prod_{j=1}^{n-1} [\mathbf{D}'_{n-j}\mathbf{F}'_{n-j}(h_{n-j})] \quad (61)$$

$$\begin{cases} \mathbf{Q}^{m(\neq n)} = \mathbf{E}_n^{-1}(0) \prod_{j=1}^{n-m-1} [\mathbf{D}_{n-j}\mathbf{F}_{n-j}(h_{n-j})]\mathbf{D}_m\mathbf{F}_m(H_m - d)\Delta_m \\ \mathbf{Q}^{m(\neq n)} = \prod_{j=1}^{n-m-1} [\mathbf{D}'_{n-j}\mathbf{F}'_{n-j}(h_{n-j})]\mathbf{D}'_m\mathbf{F}'_m(H_m - d)\Delta'_m \end{cases} \quad (62)$$

and

$$\begin{cases} \mathbf{Q}^{m(=n)} = e^{-(d-H_{n-1})\xi}\mathbf{E}_n^{-1}(0)\mathbf{Y}^s(H_{n-1} - d; n) \\ \mathbf{Q}^{m(=n)} = e^{-(d-H_{n-1})\xi}\mathbf{Y}'^s(H_{n-1} - d; n) \end{cases} \quad (63)$$

The matrix equations (60)–(63) are formally the same as those for shear faulting in Fukahata & Matsu'ura (2005).

If we take  $z = H_j$  as the reference depth in the representation of displacement potentials  $\Phi_{1j}^g$ ,  $\Phi_{2j}^g$  and  $\Psi_j^g$  instead of  $z = H_{j-1}$ , we obtain the up-going expressions of the generalized propagator matrices:

$$\bar{\mathbf{F}}_j(z) \equiv \mathbf{E}_j(-z)\mathbf{E}_j^{-1}(0), \quad \bar{\mathbf{F}}'_j(z) \equiv \mathbf{E}'_j(-z)\mathbf{E}'_j^{-1}(0) = \mathbf{E}'_j(-z). \quad (64)$$

The upgoing propagator matrices  $\bar{\mathbf{F}}_j(z)$  and  $\bar{\mathbf{F}}'_j(z)$  are related with the down-going propagator matrices  $\mathbf{F}_j(z)$  and  $\mathbf{F}'_j(z)$  in eq. (54), respectively, as

$$\bar{\mathbf{F}}_j(z) = \mathbf{F}_j(-z) = \mathbf{F}_j^{-1}(z), \quad \bar{\mathbf{F}}'_j(z) = \mathbf{F}'_j(-z) = \mathbf{F}'_j^{-1}(z). \quad (65)$$

Using the up-going propagator matrices, we can connect the deformation matrices from the bottom to the top in the up-going way, and obtain the matrix equations parallel to eq. (60):

$$\mathbf{Y}^0 = \bar{\mathbf{P}}\mathbf{A}_n + \bar{\mathbf{Q}}^m, \quad \mathbf{Y}'^0 = \bar{\mathbf{P}}'\mathbf{A}'_n + \bar{\mathbf{Q}}'^m \quad (66)$$

with

$$\bar{\mathbf{P}} = \mathbf{G}^{-1} \prod_{j=1}^{n-1} [\mathbf{F}_j(-h_j)\mathbf{D}_j^{-1}]\mathbf{E}_n(0), \quad \bar{\mathbf{P}}' = \prod_{j=1}^{n-1} [\mathbf{F}'_j(-h_j)\mathbf{D}'_j^{-1}] \quad (67)$$

$$\begin{cases} \bar{\mathbf{Q}}^{m(\neq n)} = \mathbf{G}^{-1} \prod_{j=1}^{m-1} [\mathbf{F}_j(-h_j)\mathbf{D}_j^{-1}]\mathbf{F}_m(H_{m-1} - d)\Delta_m \\ \bar{\mathbf{Q}}^{m(\neq n)} = \prod_{j=1}^{m-1} [\mathbf{F}'_j(-h_j)\mathbf{D}'_j^{-1}]\mathbf{F}'_m(H_{m-1} - d)\Delta'_m \end{cases} \quad (68)$$

and

$$\begin{cases} \bar{\mathbf{Q}}^{n(=m)} = e^{-(d-H_{n-1})\xi} \mathbf{G}^{-1} \prod_{j=1}^{n-1} [\mathbf{F}_j(-h_j) \mathbf{D}_j^{-1}] \mathbf{Y}^s(H_{n-1} - d; n) \\ \bar{\mathbf{Q}}^{n(=m)} = e^{-(d-H_{n-1})\xi} \prod_{j=1}^{n-1} [\mathbf{F}'_j(-h_j) \mathbf{D}'_j^{-1}] \mathbf{Y}'^s(H_{n-1} - d; n) \end{cases} \quad (69)$$

The matrix equations (66)–(69) are formally the same as those for shear faulting in Fukahata & Matsu'ura (2005).

### 3.3 Internal deformation fields

As shown in Fukahata & Matsu'ura (2005), we can solve eq. (60) for the deformation vectors at the Earth's surface ( $\mathbf{y}_1^0$ ,  $\mathbf{y}_2^0$  and  $\mathbf{y}_1^0$ ) by eliminating the potential coefficients in the substratum ( $\mathbf{a}_n$ ,  $\mathbf{b}_n$  and  $\mathbf{c}_n$ ) as

$$\begin{pmatrix} \mathbf{y}_1^0 \\ \mathbf{y}_2^0 \end{pmatrix} = \frac{1}{\delta} \begin{bmatrix} (P_{22} + P_{42})(\mathbf{q}_1^m + \mathbf{q}_3^m) - (P_{12} + P_{32})(\mathbf{q}_2^m + \mathbf{q}_4^m) \\ -(P_{21} + P_{41})(\mathbf{q}_1^m + \mathbf{q}_3^m) + (P_{11} + P_{31})(\mathbf{q}_2^m + \mathbf{q}_4^m) \end{bmatrix}, \quad \mathbf{y}'_1 = \frac{1}{\delta'} (\mathbf{q}'_1 + \mathbf{q}'_2) \quad (70)$$

with

$$\delta = (P_{11} + P_{31})(P_{22} + P_{42}) - (P_{12} + P_{32})(P_{21} + P_{41}), \quad \delta' = P'_{11} + P'_{21}. \quad (71)$$

On the other hand, eliminating the deformation vectors  $\mathbf{y}_1^0$ ,  $\mathbf{y}_2^0$  and  $\mathbf{y}_1^0$  in eq. (66), we obtain the potential coefficients  $\mathbf{a}_n$ ,  $\mathbf{b}_n$  and  $\mathbf{c}_n$  as

$$\begin{pmatrix} \mathbf{a}_n \\ \mathbf{b}_n \end{pmatrix} = \frac{1}{\bar{\delta}} \begin{bmatrix} -(\bar{P}_{42} - \bar{P}_{44})\bar{\mathbf{q}}_3^m + (\bar{P}_{32} - \bar{P}_{34})\bar{\mathbf{q}}_4^m \\ (\bar{P}_{41} - \bar{P}_{43})\bar{\mathbf{q}}_3^m - (\bar{P}_{31} - \bar{P}_{33})\bar{\mathbf{q}}_4^m \end{bmatrix}, \quad \mathbf{c}_n = -\frac{1}{\bar{\delta}'} \bar{\mathbf{q}}_2^m \quad (72)$$

with

$$\bar{\delta} = (\bar{P}_{31} - \bar{P}_{33})(\bar{P}_{42} - \bar{P}_{44}) - (\bar{P}_{32} - \bar{P}_{34})(\bar{P}_{41} - \bar{P}_{43}), \quad \bar{\delta}' = \bar{P}'_{21} - \bar{P}'_{22}. \quad (73)$$

Here,  $P_{ij}^{(\prime)}$  and  $\bar{P}_{ij}^{(\prime)}$  are the  $ij$ -components of  $\mathbf{P}^{(\prime)}$  and  $\bar{\mathbf{P}}^{(\prime)}$ , respectively, and  $\mathbf{q}_i^{(\prime)}$  and  $\bar{\mathbf{q}}_i^{(\prime)}$  are the  $i$ th rows of  $\mathbf{Q}^{(\prime)}$  and  $\bar{\mathbf{Q}}^{(\prime)}$ , respectively.

We have derived two different types of solutions  $\mathbf{Y}^{(0)}$  in eq. (70) and  $\mathbf{A}_n^{(0)}$  in eq. (72). Using either type of solutions, we can obtain the expressions for the deformation matrices  $\mathbf{Y}^E$  and  $\mathbf{Y}'^E$  at any depth, but they are not always numerically stable, because the  $\xi$ -dependent exponential factors in the deformation matrices diverge at  $\xi \rightarrow \infty$  in some cases (Fukahata & Matsu'ura 2005). In the substratum ( $H_{n-1} \leq z$ ) we choose the second type of solutions to obtain the proper (numerically stable) expressions:

$$\begin{cases} \mathbf{Y}^E(z; n) = \mathbf{E}_n(z - H_{n-1})\mathbf{A}_n + \delta_{mn} \exp(-|z - d| \xi) \mathbf{Y}^s(z - d; n) \\ \mathbf{Y}'^E(z; n) = \mathbf{E}'_n(z - H_{n-1})\mathbf{A}'_n + \delta_{mn} \exp(-|z - d| \xi) \mathbf{Y}'^s(z - d; n) \end{cases} \quad (74)$$

In the layers overlying the substratum, if the computation point is shallower than the source depth ( $0 \leq z < d$ ), we choose the first type of solutions to obtain the proper expressions:

$$\begin{cases} \mathbf{Y}^E(z; j) = \mathbf{F}_j(z - H_{j-1}) \prod_{k=1}^{j-1} [\mathbf{D}_{j-k} \mathbf{F}_{j-k}(h_{j-k})] \mathbf{G} \mathbf{Y}^0 \\ \mathbf{Y}'^E(z; j) = \mathbf{F}'_j(z - H_{j-1}) \prod_{k=1}^{j-1} [\mathbf{D}'_{j-k} \mathbf{F}'_{j-k}(h_{j-k})] \mathbf{Y}'^0 \end{cases} \quad (75)$$

and if the computation point is deeper than the source depth ( $d < z < H_{n-1}$ ), we choose the second type of solutions to obtain the proper expressions:

$$\begin{cases} \mathbf{Y}^E(z; j) = \mathbf{F}_j(z - H_j) \mathbf{D}_j^{-1} \prod_{k=j+1}^{n-1} [\mathbf{F}_k(-h_k) \mathbf{D}_k^{-1}] \mathbf{E}_n(0) \mathbf{A}_n \\ \mathbf{Y}'^E(z; j) = \mathbf{F}'_j(z - H_j) \mathbf{D}'_j^{-1} \prod_{k=j+1}^{n-1} [\mathbf{F}'_k(-h_k) \mathbf{D}'_k^{-1}] \mathbf{A}'_n \end{cases} \quad (76)$$

Substituting the solutions  $\mathbf{Y}^0$  and  $\mathbf{Y}'^0$  in eq. (70) or  $\mathbf{A}_n$  and  $\mathbf{A}'_n$  in eq. (72) into eqs (74)–(76), we can finally obtain the definite expressions for  $\mathbf{Y}^E$  and  $\mathbf{Y}'^E$  in the following concise forms:

$$\begin{cases} \mathbf{Y}^E(z; j) = \exp(-q\xi) \mathbf{S}_{jm}(z) + \delta_{jn} \delta_{mn} \exp(-|z - d| \xi) \mathbf{Y}^s(z - d; n) \\ \mathbf{Y}'^E(z; j) = \exp(-q\xi) \mathbf{S}'_{jm}(z) + \delta_{jn} \delta_{mn} \exp(-|z - d| \xi) \mathbf{Y}'^s(z - d; n) \end{cases} \quad (77)$$

with

$$q = \begin{cases} |z - d| & (j \neq n \text{ or } m \neq n) \\ z + d - 2H_{n-1} & (j = m = n) \end{cases} \quad (78)$$

The explicit expressions for  $\mathbf{S}_{jm}$  and  $\mathbf{S}'_{jm}$  are given in the appendix of Fukahata & Matsu'ura (2006), where the source-dependent matrices  $\mathbf{Y}^s$  and  $\Delta$  in  $\mathbf{Q}^m$  and  $\bar{\mathbf{Q}}^m$  should be replaced with  $\mathbf{Y}^s$  in eq. (44) and  $\Delta_m$  in eq. (58), respectively. Furthermore, it should be noted that the

generalized propagator matrices  $\mathbf{F}(z)$ ,  $\mathbf{F}'(z)$  and  $\mathbf{E}(z)$  in Fukahata & Matsu'ura (2006) are different from those in Fukahata & Matsu'ura (2005) and the present paper but only in the  $\xi$ -dependent exponential factor  $\exp(|z|\xi)$ .

#### 4 VISCOELASTIC SOLUTION FOR A LAYERED HALF-SPACE

We now consider the case where the  $l$ th layer of the layered half-space is viscoelastic. The rheological property of the viscoelastic layer is assumed to be Maxwell in shear and elastic in bulk:

$$\sigma_{kk} = 3K_l \varepsilon_{kk}, \quad \frac{\partial}{\partial t} \sigma'_{ij} + \frac{\mu_l}{\eta_l} \sigma'_{ij} = 2\mu_l \frac{\partial}{\partial t} \varepsilon'_{ij}, \tag{79}$$

where  $\eta_l$  denotes the viscosity of the  $l$ th layer. Performing the Laplace transformation of eq. (79), we obtain a relation between the Laplace transforms of stress and strain tensors, which is formally identical with the constitutive equation of elastic media in eq. (1):

$$\tilde{\sigma}_{kk} = 3K_l \tilde{\varepsilon}_{kk}, \quad \tilde{\sigma}'_{ij} = 2\hat{\mu}_l(s) \tilde{\varepsilon}'_{ij}. \tag{80}$$

Here,  $s$  is the Laplace transform variable, the tilde denotes the Laplace transform of the corresponding physical quantity, and  $\hat{\mu}_l(s)$  is the Laplace operator defined by

$$\hat{\mu}_l(s) = \frac{\mu_l s}{s + 1/\tau_l} \quad \text{with} \quad \tau_l = \frac{\eta_l}{\mu_l}. \tag{81}$$

The Laplace operator  $\hat{\gamma}_l(s)$  corresponding to  $\gamma_l = (3K_l + \mu_l)/(3K_l + 4\mu_l)$ , which is used in the description of elastic solution, is obtained from eq. (81) as

$$\hat{\gamma}_l(s) = \frac{\gamma_l s + 1/\nu_l}{s + 1/\nu_l} \quad \text{with} \quad \nu_l = \frac{3\tau_l}{4\gamma_l - 1}. \tag{82}$$

Here, it should be noted that the parameters  $\tau_l$  and  $\nu_l$  in eqs (81) and (82) have the dimension of time.

Then, applying the correspondence principle of linear viscoelasticity (Lee 1955; Radok 1957), we can directly obtain viscoelastic solution  $\tilde{u}_{r(\varphi,z)}^V$  in the  $s$ -domain from the associated elastic solution  $u_{r(\varphi,z)}^E$  by replacing  $\mu_l$  and  $\gamma_l$  with  $\hat{\mu}_l(s)$  and  $\hat{\gamma}_l(s)$  and the source time function  $H(t)$  with its Laplace transform  $1/s$ . Hereafter, for convenience, we represent the  $\mu_l$ - and  $\gamma_l$ -dependence of the deformation matrices  $\mathbf{Y}^E$  and  $\mathbf{Y}'^E$  explicitly. Since the source vectors  $\mathbf{j}$  and  $\mathbf{j}'$  do not contain any elastic modulus, the viscoelastic solution  $\tilde{u}_{r(\varphi,z)}^V$  in the  $s$ -domain can be written as

$$\begin{cases} \tilde{u}_r^V(r, \varphi, z, s; j) = \frac{1}{4\pi} \int_0^\infty \left[ \tilde{\mathbf{y}}_1^V(z, s; \xi; j) \frac{\partial}{\partial r} \mathbf{j}(r, \varphi; \xi) + \tilde{\mathbf{y}}_1'^V(z, s; \xi; j) \frac{1}{r} \frac{\partial}{\partial \varphi} \mathbf{j}'(r, \varphi; \xi) \right] d\xi \\ \tilde{u}_\varphi^V(r, \varphi, z, s; j) = \frac{1}{4\pi} \int_0^\infty \left[ \tilde{\mathbf{y}}_1^V(z, s; \xi; j) \frac{1}{r} \frac{\partial}{\partial \varphi} \mathbf{j}(r, \varphi; \xi) - \tilde{\mathbf{y}}_1'^V(z, s; \xi; j) \frac{\partial}{\partial r} \mathbf{j}'(r, \varphi; \xi) \right] d\xi \\ \tilde{u}_z^V(r, \varphi, z, s; j) = \frac{1}{4\pi} \int_0^\infty \tilde{\mathbf{y}}_2^V(z, s; \xi; j) \mathbf{j}(r, \varphi; \xi) \xi d\xi \end{cases} \tag{83}$$

with

$$\tilde{\mathbf{y}}_{1(2)}^V(z, s; \xi; j) = \frac{1}{s} \mathbf{y}_{1(2)}^E(z; \xi; j; \hat{\mu}_l, \hat{\gamma}_l), \quad \tilde{\mathbf{y}}_1'^V(z, s; \xi; j) = \frac{1}{s} \mathbf{y}_1'^E(z; \xi; j; \hat{\mu}_l). \tag{84}$$

Here, the  $s$ -dependent deformation vectors  $\mathbf{y}_k^E(z; j; \hat{\mu}_l; \hat{\gamma}_l)$  and  $\mathbf{y}_k'^E(z; j; \hat{\mu}_l)$  are the  $k$ th rows of the  $s$ -dependent deformation matrices  $\mathbf{Y}^E(z; j; \hat{\mu}_l, \hat{\gamma}_l)$  and  $\mathbf{Y}'^E(z; j; \hat{\mu}_l)$ , respectively, which are directly obtained from  $\mathbf{Y}^E$  and  $\mathbf{Y}'^E$  in eqs (74)–(76) by replacing  $\mu_l$  and  $\gamma_l$  with  $\hat{\mu}_l(s)$  and  $\hat{\gamma}_l(s)$ ; that is, if the substratum is viscoelastic ( $l = n$ ),

$$\begin{cases} \mathbf{Y}^E(z; j; \hat{\mu}_n, \hat{\gamma}_n) = \exp(-q\xi) \mathbf{S}_{jm}(z; \hat{\mu}_n, \hat{\gamma}_n) + \delta_{jn} \delta_{mn} \exp(-|z-d|\xi) \mathbf{Y}^s(z-d; n; \hat{\gamma}_n) \\ \mathbf{Y}'^E(z; j; \hat{\mu}_n) = \exp(-q\xi) \mathbf{S}'_{jm}(z; \hat{\mu}_n) + \delta_{jn} \delta_{mn} \exp(-|z-d|\xi) \mathbf{Y}'^s(z-d; n) \end{cases}, \tag{85}$$

and otherwise

$$\begin{cases} \mathbf{Y}^E(z; j; \hat{\mu}_l, \hat{\gamma}_l) = \exp(-q\xi) \mathbf{S}_{jm}(z; \hat{\mu}_l, \hat{\gamma}_l) + \delta_{jn} \delta_{mn} \exp(-|z-d|\xi) \mathbf{Y}^s(z-d; n; \gamma_n) \\ \mathbf{Y}'^E(z; j; \hat{\mu}_l) = \exp(-q\xi) \mathbf{S}'_{jm}(z; \hat{\mu}_l) + \delta_{jn} \delta_{mn} \exp(-|z-d|\xi) \mathbf{Y}'^s(z-d; n) \end{cases}. \tag{86}$$

From eqs (44) and (82) we can see that the matrix  $\mathbf{Y}^s(z-d; n; \hat{\gamma}_n)$  in eq. (85) has the form of a rational function of first-degree polynomials in  $s$ :

$$\mathbf{Y}^s(z-d; n; \hat{\gamma}_n) = \frac{1}{s + 1/\nu_n} \left[ s \mathbf{Y}^s(z-d; n; \gamma_n) + \frac{1}{\nu_n} \mathbf{Y}^s(z-d; n; \gamma_n = 1) \right]. \tag{87}$$

The matrix  $\mathbf{S}_{jm}^{(l)}$ , defined by the products of plural matrices, contains the  $\gamma_l$ -dependent matrices [ $\mathbf{\Delta}_m$  (if  $m = l$ ),  $\mathbf{E}_n(0)$  and  $\mathbf{E}_n^{-1}(0)$  (if  $n = l$ ), and  $\mathbf{F}_l$ ] and the  $\mu_l$ -dependent matrices [ $\mathbf{G}$  and  $\mathbf{G}^{-1}$  (if  $l = 1$ ),  $\mathbf{D}_l^{(l)}$ ,  $\mathbf{D}_l^{(l)-1}$ ,  $\mathbf{D}_{l-1}^{(l)}$  and  $\mathbf{D}_{l-1}^{(l)-1}$ ]. For the  $\gamma_l$ -dependent matrices, replacing  $\gamma_l$  with  $\hat{\gamma}_l(s)$ , we obtain the corresponding  $s$ -dependent matrices in the form of

$$\mathbf{B}(\hat{\gamma}_l) = \frac{1}{s + 1/\nu_l} \left[ s \mathbf{B}(\gamma_l) + \frac{1}{\nu_l} \mathbf{B}(\gamma_l = 1) \right]. \tag{88}$$

For the  $\mu_l$ -dependent matrices, replacing  $\mu_l$  with  $\hat{\mu}_l(s)$ , we obtain the corresponding  $s$ -dependent matrices in the form of

$$\mathbf{B}(\hat{\mu}_l) = \frac{1}{s + 1/\tau_l} \left[ s\mathbf{B}(\mu_l) + \frac{1}{\tau_l} \mathbf{B}(\mu_l = 0) \right]. \quad (89)$$

When  $\mu_l$  appears in the form of  $1/\mu_l$ , the limit of  $1/\mu_l$  at  $\mu_l \rightarrow 0$  diverges. In this case, instead of eq. (89), we use the following formula to obtain the corresponding  $s$ -dependent matrices:

$$\mathbf{B}(\hat{\mu}_l) = \frac{1}{s} \left\{ s\mathbf{B}(\mu_l) + \frac{1}{2\tau_l} [\mathbf{B}(\mu_l) - \mathbf{B}(-\mu_l)] \right\}. \quad (90)$$

Therefore, as shown in Fukahata & Matsu'ura (2006), the  $s$ -dependent deformation matrices  $\mathbf{Y}^E(z; j; \hat{\mu}_l, \hat{\gamma}_l)$  and  $\mathbf{Y}'^E(z; j; \hat{\mu}_l)$  can be expressed in the form of a rational function of  $s$  as

$$\mathbf{Y}^E(z; j; \hat{\mu}_l, \hat{\gamma}_l) = \frac{\sum_{i=0}^M \mathbf{A}_i s^i}{\sum_{i=0}^M b_i s^i}, \quad \mathbf{Y}'^E(z; j; \hat{\mu}_l) = \frac{\sum_{i=0}^{M'} \mathbf{A}'_i s^i}{\sum_{i=0}^{M'} b'_i s^i}. \quad (91)$$

Then, the  $s$ -dependent deformation vectors  $\mathbf{y}_k^E(z; j; \hat{\mu}_l, \hat{\gamma}_l)$  and  $\mathbf{y}'_k^E(z; j; \hat{\mu}_l)$ , which are the  $k$ th rows of  $\mathbf{Y}^E(z; j; \hat{\mu}_l, \hat{\gamma}_l)$  and  $\mathbf{Y}'^E(z; j; \hat{\mu}_l)$ , can also be expressed in the form of a rational function:

$$\mathbf{y}_k^E(z; j; \hat{\mu}_l, \hat{\gamma}_l) = \frac{\sum_{i=0}^M \mathbf{a}_{ki} s^i}{\sum_{i=0}^M b_i s^i}, \quad \mathbf{y}'_k^E(z; j; \hat{\mu}_l) = \frac{\sum_{i=0}^{M'} \mathbf{a}'_{ki} s^i}{\sum_{i=0}^{M'} b'_i s^i} \quad (92)$$

with

$$\frac{\mathbf{a}_{kM}}{b_M} = \mathbf{y}_k^E(z; j; \mu_l, \gamma_l), \quad \frac{\mathbf{a}'_{kM'}}{b'_{M'}} = \mathbf{y}'_k^E(z; j; \mu_l). \quad (93)$$

Here, it should be noted that the degrees  $M$  and  $M'$  of the polynomials for the deformation vectors depend on the case. For example, when the source is located in one of the elastic layers ( $m \neq l$ ) overlying the viscoelastic substratum ( $l = n$ ), the degrees of polynomials are  $M = 3$  and  $M' = 1$ . When the viscoelastic layer without sources intervenes between elastic layers ( $l \neq m, n$ ), the degrees of polynomials are  $M = 6$  and  $M' = 2$  (Matsu'ura *et al.* 1981). If the number of viscoelastic layers is more than one, this procedure becomes more complicated (Sato & Matsu'ura 1993). General treatment in such a case is given in Fukahata & Matsu'ura (2006).

Given the explicit expressions for the  $s$ -dependent deformation vectors,  $\mathbf{y}_k^E(z; j; \hat{\mu}_l, \hat{\gamma}_l)$  and  $\mathbf{y}'_k^E(z; j; \hat{\mu}_l)$  in the form of rational functions, we can obtain the viscoelastic solution in the time domain by using the algorithm developed by Matsu'ura *et al.* (1981) as follows. First, with division algorithm and partial fraction resolution, we rewrite  $\tilde{\mathbf{y}}_k^V(z, s; \xi; j)$  and  $\tilde{\mathbf{y}}_k'^V(z, s; \xi; j)$  in eq. (84) as

$$\begin{cases} \tilde{\mathbf{y}}_k^V(z, s; \xi; j) = \frac{1}{s} \mathbf{y}_k^E(z; \xi; j; \mu_l, \gamma_l) - \sum_{i=1}^M \mathbf{v}_{ki}(\xi) \left[ \frac{1}{s} - \frac{1}{s - \zeta_i(\xi)} \right] \\ \tilde{\mathbf{y}}_k'^V(z, s; \xi; j) = \frac{1}{s} \mathbf{y}'_k^E(z; \xi; j; \mu_l) - \sum_{i=1}^{M'} \mathbf{v}'_{ki}(\xi) \left[ \frac{1}{s} - \frac{1}{s - \zeta'_i(\xi)} \right] \end{cases} \quad (94)$$

with

$$\begin{cases} \mathbf{v}_{ki}(\xi) = \frac{1}{b_M(\xi)\zeta_i(\xi)} \prod_{j=1(j \neq i)}^M \frac{1}{\zeta_i(\xi) - \zeta_j(\xi)} \sum_{j=0}^M \mathbf{a}_{kj}(\xi) \zeta_i^j(\xi) \\ \mathbf{v}'_{ki}(\xi) = \frac{1}{b'_{M'}(\xi)\zeta'_i(\xi)} \prod_{j=1(j \neq i)}^{M'} \frac{1}{\zeta'_i(\xi) - \zeta'_j(\xi)} \sum_{j=0}^{M'} \mathbf{a}'_{kj}(\xi) \zeta_i'^j(\xi) \end{cases}, \quad (95)$$

where  $\zeta_i(\xi)$  and  $\zeta'_i(\xi)$  denote the roots of algebraic equations  $\sum_{i=0}^M b_i(\xi)s^i = 0$  and  $\sum_{i=0}^{M'} b'_i(\xi)s^i = 0$ , respectively, which are always real-negative. Next, performing the inverse Laplace transformation of eq. (94), we obtain the expressions for the deformation vectors in the time domain as

$$\begin{cases} \mathbf{y}_k^V(z, t; \xi; j) = H(t) \mathbf{y}_k^E(z; \xi; j; \mu_l, \gamma_l) - H(t) \sum_{i=1}^M \mathbf{v}_{ki}(\xi) [1 - e^{\zeta_i(\xi)t}] \\ \mathbf{y}'_k^V(z, t; \xi; j) = H(t) \mathbf{y}'_k^E(z; \xi; j; \mu_l) - H(t) \sum_{i=1}^{M'} \mathbf{v}'_{ki}(\xi) [1 - e^{\zeta'_i(\xi)t}] \end{cases}. \quad (96)$$

Here, the first terms on the right-hand side of the above equations represent the instantaneous elastic deformation, and the second terms the transient deformation due to viscoelastic stress relaxation. Finally, replacing  $\tilde{\mathbf{y}}_k^V(z, s; \xi; j)$  and  $\tilde{\mathbf{y}}_k'^V(z, s; \xi; j)$  in eq. (83) with  $\mathbf{y}_k^V(z, t; \xi; j)$  and  $\mathbf{y}'_k^V(z, t; \xi; j)$  in eq. (96), respectively, we obtain the expressions for viscoelastic displacements in the time domain:

$$u_{r(\varphi, z)}^V(r, \varphi, z, t; j) = u_{r(\varphi, z)}^E(r, \varphi, z, t; j) + u_{r(\varphi, z)}^T(r, \varphi, z, t; j), \quad (97)$$

where  $u_{r(\varphi, z)}^E$  are the instantaneous elastic responses obtained in Section 3, and  $u_{r(\varphi, z)}^T$  are the transient responses due to viscoelastic stress relaxation, represented by the superposition of exponentially decaying modes with the  $\xi$ -dependent relaxation times of  $1/|\zeta_i(\xi)|$  or

$1/|\zeta'_i(\xi)|$ :

$$\begin{cases} u_r^T(r, \varphi, z, t; j) = -\frac{H(t)}{4\pi} \left[ \sum_{i=1}^M \int_0^\infty \mathbf{v}_{1i}(\xi) \frac{\partial}{\partial r} \mathbf{j}(r, \varphi; \xi) T_i(t; \xi) d\xi + \sum_{i=1}^{M'} \int_0^\infty \mathbf{v}'_{1i}(\xi) \frac{1}{r} \frac{\partial}{\partial \varphi} \mathbf{j}'(r, \varphi; \xi) T'_i(t; \xi) d\xi \right] \\ u_\varphi^T(r, \varphi, z, t; j) = -\frac{H(t)}{4\pi} \left[ \sum_{i=1}^M \int_0^\infty \mathbf{v}_{1i}(\xi) \frac{1}{r} \frac{\partial}{\partial \varphi} \mathbf{j}(r, \varphi; \xi) T_i(t; \xi) d\xi + \sum_{i=1}^{M'} \int_0^\infty \mathbf{v}'_{1i}(\xi) \frac{\partial}{\partial r} \mathbf{j}'(r, \varphi; \xi) T'_i(t; \xi) d\xi \right] \\ u_z^T(r, \varphi, z, t; j) = -\frac{H(t)}{4\pi} \sum_{i=1}^M \int_0^\infty \mathbf{v}_{2i}(\xi) \mathbf{j}(r, \varphi; \xi) T_i(t; \xi) \xi d\xi \end{cases} \quad (98)$$

with

$$T_i(t; \xi) = 1 - \exp[-\zeta_i(\xi)t], \quad T'_i(t; \xi) = 1 - \exp[\zeta'_i(\xi)t]. \quad (99)$$

### 5 NUMERICAL EXAMPLES

In the previous sections we derived the expressions for the quasi-static internal displacement fields due to a moment tensor in an elastic/viscoelastic multilayered half-space under gravity. In order to obtain the displacement fields due to a finite-dimensional source we numerically integrate the point source solutions over the source region. In the present section, as numerical examples, we show the quasi-static internal displacement fields associated with dyke intrusion, episodic segmental ridge opening and steady plate divergence in the case of an elastic–viscoelastic two-layered half-space. The values of structural parameters used for computation are given in Table 1. The coordinate system and crack geometry are shown in Fig. 3, where the rectangle represents a vertical tensile crack with length  $L$  and width  $W$ . We also demonstrate the usefulness of the source representation with moment tensor through the numerical simulation of deformation cycles associated with the periodic occurrence of interplate strike-slip earthquakes in a ridge-transform fault system. Further numerical examples for shear faulting are given in Fukahata & Matsu’ura (2006).

At the moment of crack opening or shear faulting, the step-response of the composite system is completely elastic. As time passes, deviatoric stress in the viscoelastic substratum gradually relaxes. Then, after the completion of the viscoelastic stress relaxation, a certain amount of permanent displacements remains. At the final stage the elastic–viscoelastic composite system behaves just like an elastic plate floating on water. In the following numerical examples we show how the patterns of displacement fields change with time and depend on the source extent.

**Table 1.** The structural parameters of the elastic–viscoelastic two-layered model used for computation

No.	Thickness	$V_p$ (km s <sup>-1</sup> )	$V_s$ (km s <sup>-1</sup> )	$\rho$ (kg m <sup>-3</sup> )	$\eta$ (Pa s)
1	$h_1$	6.0	3.5	$3.0 \times 10^3$	$\infty$
2	$\infty$	7.0	4.0	$3.3 \times 10^3$	$1 \times 10^{19}$

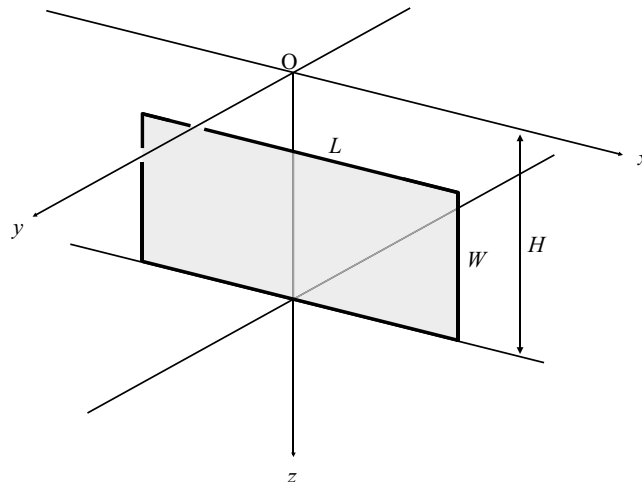


**Figure 3.** The coordinate system and crack geometry in numerical computation. The rectangle represents a vertical tensile crack with length  $L$  and width  $W$  in the elastic surface layer overlying a viscoelastic half-space.

#### 5.1 Dyke intrusion

First, we consider the sudden opening of a 10-km-long vertical crack embedded in a 20-km-thick elastic surface layer with different depths to the top. The bottom of the crack reaches down to the elastic–viscoelastic layer interface. The depth to the crack top is taken to be 15, 10, 5 and

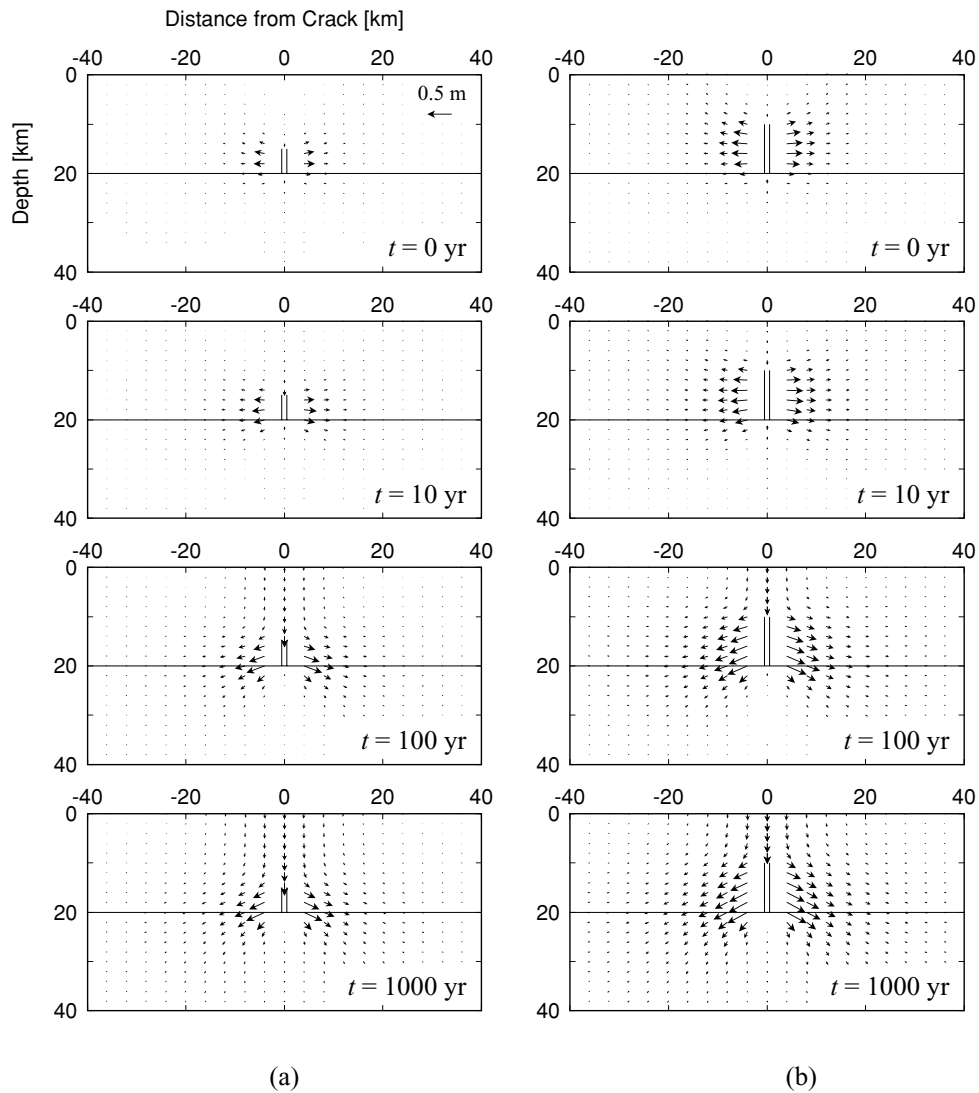


**Figure 4.** Temporal change of internal displacement fields due to the sudden opening of a 10-km-long vertical crack embedded in the 20-km-thick elastic surface layer with different depths to the top. The vertical cross-sections of the internal displacement fields at the centre of the 10-km-long crack are shown in the cases of (a)  $W = 5$  km, (b)  $W = 10$  km, (c)  $W = 15$  km and (d)  $W = 20$  km. The double solid line represents the vertical section of the crack. The values of structural parameters used for computation are given in Table 1.

0 km, which correspond to the cases (a), (b), (c) and (d) in Fig. 4, respectively. This numerical example may be compared to dyke intrusion. In each case we show the vertical cross-sections of internal displacement fields at  $t = 0, 10, 100$  and  $1000$  yr after the crack opening. In either case of (a), (b) and (c) where the crack is buried under the Earth’s surface, we can observe divergent horizontal displacements due to crack opening at the early stage. As time passes, the region surrounding the crack gradually subsides because of the viscoelastic stress relaxation in the substratum. This deformation pattern can be interpreted as the downward bending of the elastic plate by crack opening at the bottom. In the case (d) where the top of the crack reaches to the Earth’s surface, the displacement fields show essentially different patterns from the previous three cases. At the early stage we can observe the broad uplift of the Earth’s surface in addition to the divergent horizontal displacements. At the latter stage, the uplift pattern holds in the upper half of the elastic surface layer, but gradually changes to subsidence in the lower half as stress relaxation proceeds in the viscoelastic substratum. Then, the deformation pattern becomes nearly symmetric with respect to the mean depth of the elastic surface layer.

### 5.2 Episodic segmental ridge opening

Second, we consider the sudden opening of a 100-km-long vertical crack that cuts through the 20-km-thick elastic surface layer overlying a viscoelastic substratum. This case may be compared to episodic segmental ridge opening, observed in Iceland for example. In Fig. 5, we show the patterns of surface horizontal displacement fields (top panel) and the vertical cross-sections of internal displacement fields (bottom panel) at the time  $t = 0, 10, 100$  and  $1000$  yr after the crack opening. From the patterns of surface horizontal displacement fields we can observe that the deformation area gradually expands in the direction perpendicular to the crack strike with time. Such diffusive crustal motion

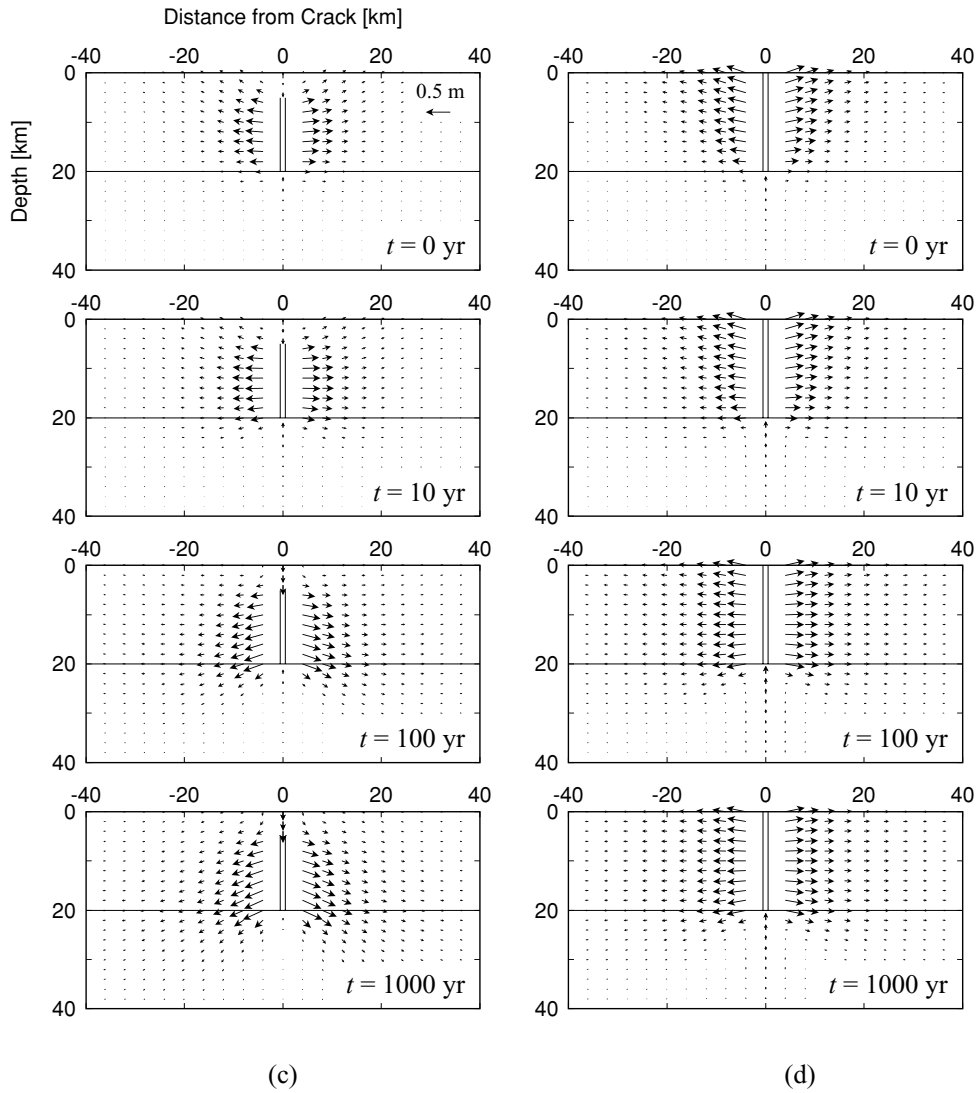


Figure 4. (Continued.)

has been observed after the episodic segmental ridge opening in Iceland (Foulger *et al.* 1992). From the vertical cross-sections of internal displacement fields we can observe the broad uplift of the Earth's surface at the early stage. As time passes, while the divergent horizontal displacements remain, the upward displacements in the elastic surface layer gradually disappear because of the viscoelastic stress relaxation in the substratum.

### 5.3 Steady plate divergence

Third, we consider the sudden opening of an infinitely long crack that divides the elastic surface layer into two plates. Here, the thickness of the elastic surface layer  $h_1$  is taken to be 10 km. The values of the other structural parameters are the same as those in the previous cases. This case may be compared to steady plate divergence, observed in mid-ocean ridges, as explained later. For the computation of displacement fields due to an infinitely long crack, we use the solution for a line source, which is obtained by integrating the solution for a point source derived in the previous section along the  $x$ -axis (Sato & Matsu'ura 1993; Fukahata & Matsu'ura 2005) as

$$\begin{cases} u_x^L(y, z, t; j) = \frac{H(t)}{4\pi} \int_0^\infty \mathbf{y}_1^V(z, t; \xi; j) \mathbf{l}_x(y; \xi) d\xi \\ u_y^L(y, z, t; j) = \frac{H(t)}{4\pi} \int_0^\infty \mathbf{y}_1^V(z, t; \xi; j) \mathbf{l}_y(y; \xi) d\xi \\ u_z^L(y, z, t; j) = \frac{H(t)}{4\pi} \int_0^\infty \mathbf{y}_2^V(z, t; \xi; j) \mathbf{l}_z(y; \xi) d\xi \end{cases} \quad (100)$$

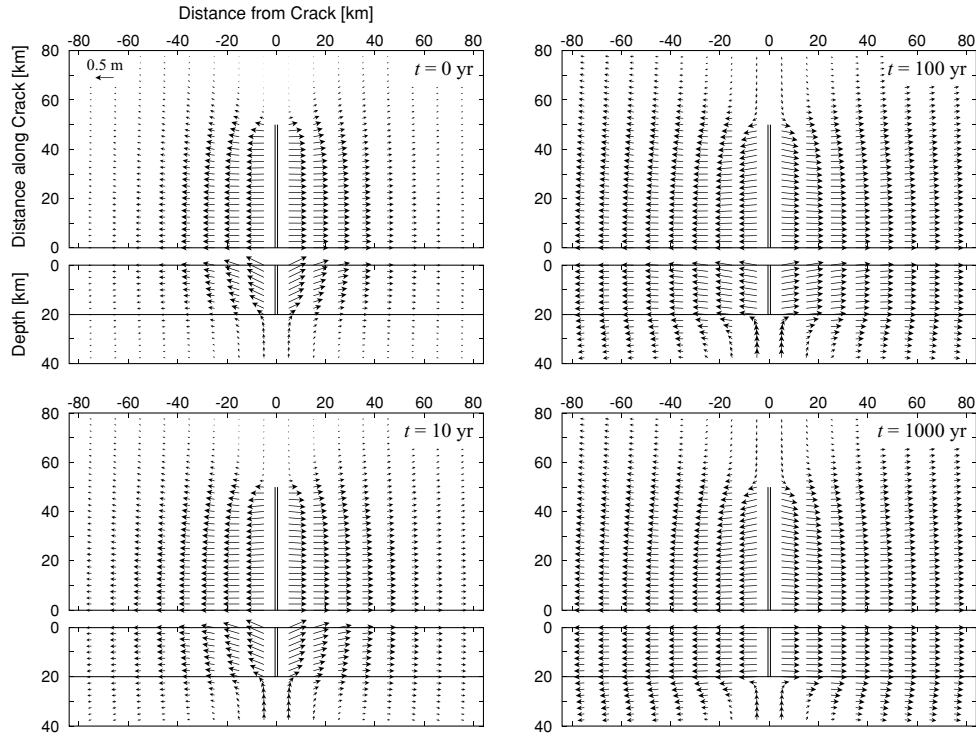


**Figure 5.** Temporal change of the surface and internal displacement fields due to the sudden opening of a 100-km-long vertical crack that cuts through the 20-km-thick elastic surface layer overlying the viscoelastic substratum. The horizontal displacement fields at the surface and the vertical cross-section of internal displacement fields at the centre of the 100-km-long crack are shown at the top and the bottom of each diagram, respectively. The double solid lines represent the horizontal and vertical sections of the crack. The values of structural parameters used for computation are given in Table 1.

with

$$\mathbf{I}'_x(y; \xi) = -2 \begin{pmatrix} m_3 \cos \xi y \\ 2m_6 \sin \xi y \end{pmatrix}, \quad \mathbf{I}'_y(y; \xi) = -2 \begin{pmatrix} m_1 \sin \xi y \\ m_2 \sin \xi y \\ -m_4 \cos \xi y \\ m_5 \sin \xi y \end{pmatrix}, \quad \mathbf{I}'_z(y; \xi) = 2 \begin{pmatrix} m_1 \cos \xi y \\ m_2 \cos \xi y \\ m_4 \sin \xi y \\ m_5 \cos \xi y \end{pmatrix}, \quad (101)$$

where the deformation vectors  $\mathbf{y}'_1^V$ ,  $\mathbf{y}'_1^V$  and  $\mathbf{y}'_2^V$  are the same as those in the case of point sources, and  $m_i$  ( $i = 1, \dots, 6$ ) are defined in eq. (27).

In Fig. 6 we show the vertical cross-sections of internal displacement fields at the time  $t = 0, 4\tau, 20\tau$  and  $20\,000\tau$ . Here,  $\tau = \eta_2/\mu_2$  denotes the characteristic time of stress relaxation in the viscoelastic substratum. The displacement fields at the early stage ( $t = 0, 4\tau$ ) are similar to those in the case of the 100-km-long crack (Fig. 5). As time passes ( $t = 20\tau$ ), the upward displacements in the elastic surface layer gradually disappear, and the divergent horizontal displacements become dominant. Unlike the case of the 100-km-long crack, the deformation area gradually expands with time to infinite distance. Then, at the final stage ( $t = 20\,000\tau$ ), we can observe the horizontally divergent rigid plate displacements, accompanied by upward displacements in the viscoelastic substratum.

In Fig. 7 we show the profiles of the horizontal and vertical components of the surface displacement fields in Fig. 6 at  $t = 0, 2\tau, 4\tau, 10\tau, 20\tau, 100\tau$  and  $20\,000\tau$ . From Fig. 7(a) we can observe that the initial divergent horizontal displacement field gradually expands from the source area to the distant region with time and finally tend to the divergent rigid plate displacements with the half value of crack opening. From Fig. 7(b), on the other hand, we can observe that the initial vertical displacements characterized by uplifts in the source area gradually decay to zero with time. Hofton & Foulger (1996) have computed the temporal change in the profiles of surface displacement fields due to crack opening in a very similar situation (sudden opening of an infinitely long vertical crack cutting through the 10-km-thick elastic surface layer with slightly different elastic constants), and so we can directly compare their results with our results in Fig. 7. In their results, the horizontal displacements overshoot the half value of crack opening at  $t = 2\tau$ , and the transition to the divergent rigid plate displacements is irregular. As for the vertical displacements (their profiles are probably upside down), the significant deformation of the elastic plate remains at  $t \rightarrow \infty$ . These discrepancies between their results and our results must come from the mathematical expressions used for numerical computation. Hofton & Foulger (1996), based on Hofton *et al.* (1995), used the up-going algorithm of the propagator matrix, which is numerically unstable at the Earth's surface. In addition, the use of an approximation technique for inverse Laplace transformation (Rundle 1982a) would also cause to the discrepancies.

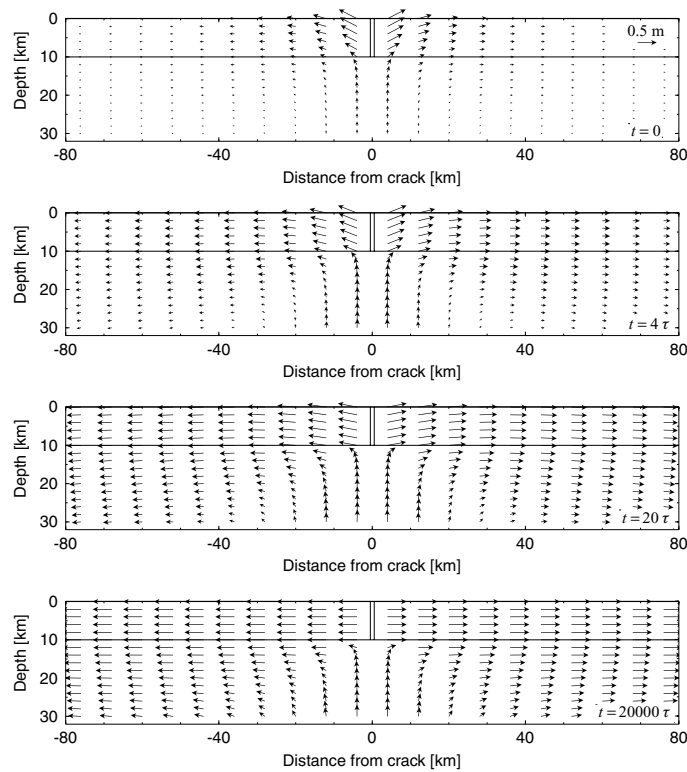


**Figure 6.** Temporal change of the internal displacement fields due to the sudden opening of an infinitely long crack that divides the 10-km-thick elastic surface layer overlying the viscoelastic substratum into two plates. The vertical cross-sections of the internal displacement fields at  $t = 0, 4\tau, 20\tau$  and  $20\,000\tau$  are shown. Here,  $\tau = \eta_2/\mu_2$  denotes the characteristic time of stress relaxation in the viscoelastic substratum. The double solid line represents the vertical section of the crack. The values of structural parameters used for computation are given in Table 1.

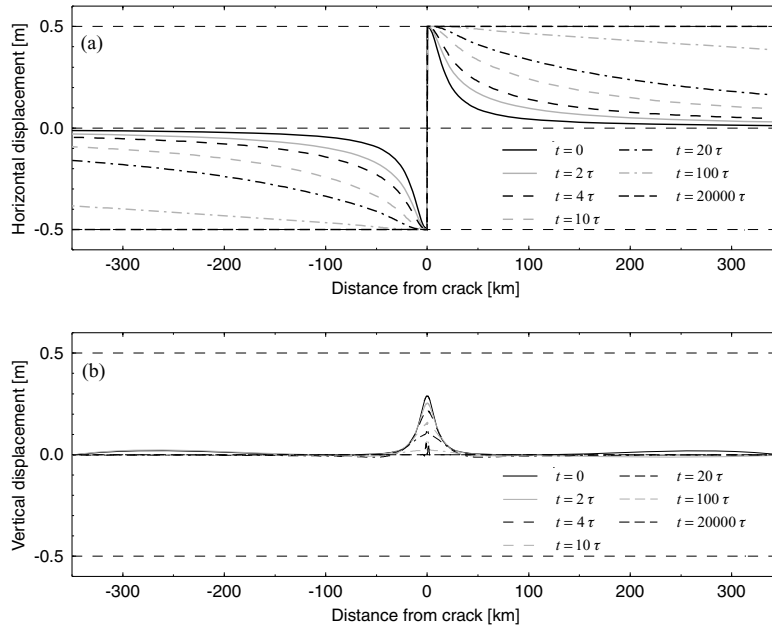


**Figure 7.** Temporal change in the profiles of the surface displacement fields due to crack opening in the same situation as in Fig. 6. (a) Horizontal components. (b) Vertical components. In both cases the displacement profiles at  $t = 0, 2\tau, 4\tau, 10\tau, 20\tau, 100\tau$  and  $20\,000\tau$  are shown. Here,  $\tau = \eta_2/\mu_2$  denotes the characteristic relaxation time in the viscoelastic substratum. We can compare these displacement profiles with those in Fig. 8 of Hofton & Foulger (1996).

The diagrams in Figs 6 and 7 show the viscoelastic responses to a unit-step crack opening. According to Matsu'ura & Sato (1989) and Sato & Matsu'ura (1993), we can read these results as the displacement rates (velocities) due to steady crack opening. Denoting the response to a unit-step crack opening over the whole plate interface at  $t = 0$  by  $U_i(\mathbf{x}, t)$ , we can express the cumulative displacements  $w_i(\mathbf{x}, t)$  due to steady crack opening at a constant rate  $V_{pl}$  for  $t \geq 0$  by using the technique of hereditary integral as

$$w_i(\mathbf{x}, t) = V_{pl} \int_0^t U_i(\mathbf{x}, t - \tau) d\tau. \quad (102)$$

Since the viscoelastic step response  $U_i(\mathbf{x}, t)$  becomes constant  $U_i(\mathbf{x}, t \rightarrow \infty)$  at the time  $t$  much longer than the effective relaxation time  $\tau_e \sim 100 \tau$  of the composite system, we can obtain the displacement rate by differentiating the both sides of eq. (102) with respect to  $t$ :

$$v_i(\mathbf{x}, t) \equiv \frac{d}{dt} w_i(\mathbf{x}, t) = V_{pl} U_i(\mathbf{x}, t \rightarrow \infty) \quad (t \gg \tau_e). \quad (103)$$

Thus, we can read the displacement fields at  $t = 20\,000 \tau$  in Figs 6 and 7 as the long-term averaged velocity fields due to steady crack opening at a constant rate.

#### 5.4 Deformation cycles in a ridge-transform fault system

Finally, we consider the deformation cycles associated with the periodic occurrence of interplate strike-slip earthquakes in the ridge-transform fault system, which is composed of two parallel semi-infinite vertical cracks extending in opposite directions and a vertical transcurrent fault that connects the semi-infinite cracks at their ends. The ridge-transform fault system divides the 10-km-thick elastic surface layer overlying a viscoelastic substratum into two plates. We suppose the steady opening of the semi-infinite cracks at a constant rate and the periodic stick-slip motion at the transcurrent fault with the interval of 100 yr. In Fig. 8 we show the temporal change of the horizontal displacement field at the Earth's surface during one earthquake cycle after many times repetition of stick-slip motion with the same interval. As the reference we took the displacement field just after the occurrence of the last earthquake ( $t = 0^+$  yr). Then, the displacement field at  $t = 100^-$  yr represents that just before the occurrence of the next earthquake. After the completion of one earthquake cycle ( $t = 100^+$  yr), unlike the deformation cycles in subduction zones (Matsu'ura & Sato 1989), we can only observe horizontally divergent rigid plate displacements. In the interseismic period ( $0^+ \leq t \leq 100^-$ ) we can observe the gradual increase of the distortion of the horizontal displacement fields around the transcurrent fault. The occurrence of a strike-slip earthquake at the transcurrent fault completely releases the distortion of the horizontal displacement field.

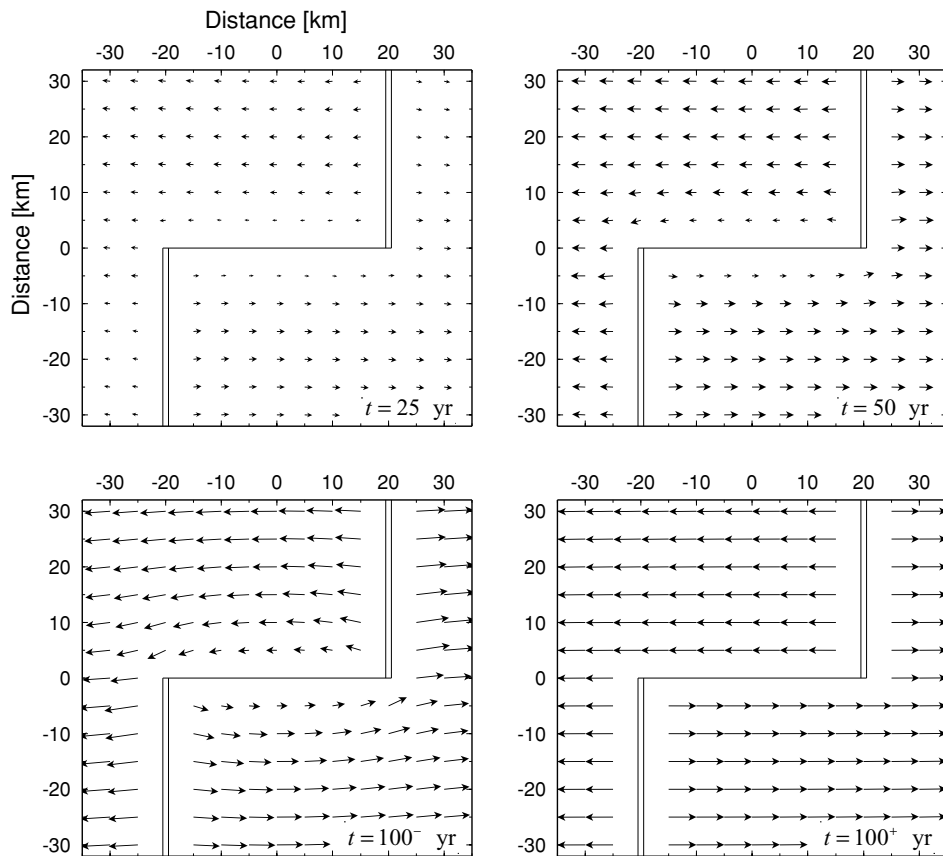


**Figure 8.** Temporal change of the surface horizontal displacement field during one earthquake cycle in the ridge-transform fault system. The ridge-transform fault system is composed of two parallel semi-infinite vertical cracks (double solid lines) and one vertical transcurrent fault (single solid line). The thickness of the elastic surface layer is taken to be 10 km. The values of the other structural parameters are given in Table 1. We suppose the steady opening of the semi-infinite cracks at a constant rate and the periodic stick-slip motion at the transcurrent fault with the interval of 100 yr. The displacement field just after the occurrence of the last earthquake ( $t = 0^+$  yr) is taken as the reference. In the interseismic period ( $0^+ \leq t \leq 100^-$ ) we can observe the gradual increase of the distortion of the horizontal displacement fields (represented by solid arrows) around the transcurrent fault. The occurrence of a strike-slip earthquake at the transcurrent fault completely releases the distortion of the horizontal displacement field. Then, after the completion of one earthquake cycle ( $t = 100^+$  yr), horizontally divergent rigid plate displacements remain.

## 6 DISCUSSION AND CONCLUSIONS

We succeeded in obtaining the expressions for internal deformation fields due to a moment tensor in an elastic/viscoelastic multilayered half-space under gravity. This is the general extension of the mathematical formulation for shear faulting by Fukahata & Matsu'ura (2005, 2006). In Section 2, we derived the expressions of static displacement potentials for a moment tensor in cylindrical coordinates. In Section 3, representing internal displacement fields by the superposition of a particular solution for a moment tensor in an infinite elastic medium and the general solution for a layered elastic half-space without sources, and using the generalized propagator matrix method developed by Fukahata & Matsu'ura (2005), we obtained the expressions for internal displacement fields due to a moment tensor in an elastic multilayered half-space. In Section 4, applying the correspondence principle of linear viscoelasticity (Lee 1955; Radok 1957) to the associated elastic solution, we obtained the general expressions for internal displacement fields due to a moment tensor in an elastic/viscoelastic multilayered half-space.

So far, in most studies, static solutions have been obtained by taking the limit of  $\omega \rightarrow 0$  for the corresponding dynamic solutions in the frequency domain. In static problems, however, the solutions derived from dynamic displacement potentials degenerate with one another (Takeuchi 1959; Sato 1971; Zhu & Rivera 2002), and so we must find a new set of displacement potentials that produces independent static solutions. In the present study, to avoid such a complicated process, we directly obtained the expressions of static displacement potentials in cylindrical coordinates by taking the limit of  $t \rightarrow \infty$  for the corresponding dynamic solution in Cartesian coordinates (Aki & Richards 1980) and performing its Hankel transformation.

In the framework of elasticity theory any indigenous source can be represented by a moment tensor (Backus & Mulcahy 1976a, b). Therefore, the general expression for a moment tensor obtained in the present study includes the internal displacement fields due to isotropic expansion, crack opening and shear faulting as special cases. The expression for shear faulting is identical with that obtained by Fukahata & Matsu'ura (2005, 2006). By adding the expressions for isotropic expansion and crack opening we completed the mathematical formulation for internal deformation fields due to indigenous sources. The general formulation with moment tensor is useful in computing internal deformation fields due to composite force systems corresponding to composite processes such as dyke intrusion with pressure increase, shear fracture with dilatancy, ridge-transform fault interaction, and ridge subduction.

As for isotropic expansion we may consider two different cases; transformational volume expansion  $\Theta$  and pressure increase  $\Delta p$  in a spherical cavity. The general expressions in Section 3 include the former case, but not the latter case. If the source is located in an elastic layer, we can directly obtain the expression for uniform pressure increase  $\Delta p$  in a spherical cavity with radius  $a$  by replacing the factor  $(4\pi a^3/3)K\Theta$  of the source vector  $\mathbf{j}$  in eq. (28) with  $(K/\mu + 4/3)\pi a^3 \Delta p$ . On the other hand, if the source is located in a viscoelastic layer, the solutions for these two sources have quite different time-dependence from each other, because the source vector  $\mathbf{j}$  in the latter case includes the rigidity  $\mu$ , which should be replaced with the  $s$ -dependent operator  $\hat{\mu}(s) = \mu s/(s + 1/\tau)$ .

The viscoelastic solution in the  $s$ -domain is directly obtained by applying the correspondence principle to the associated elastic solution. In order to obtain the viscoelastic solution in the time domain we must perform the inverse Laplace transformation of the solution in the  $s$ -domain. This is a difficult problem. For example, Rundle and his co-workers (Rundle 1978, 1982a; Hofton *et al.* 1995) have introduced an approximation technique to perform the inverse Laplace transform. Wang *et al.* (2006), who handled the problem in the Fourier transform domain instead of the Laplace transform domain, have developed an approximation technique to perform the inverse Fourier transform. We performed the inverse Laplace transformation in an exact way by using the algorithm developed by Matsu'ura *et al.* (1981).

## ACKNOWLEDGMENTS

We thank Massimo Cocco and anonymous reviewers for their useful comments and suggestions to improve our manuscript.

## REFERENCES

- Aki, K. & Richards, P.G., 1980. *Quantitative Seismology: Theory and Methods*, W.H. Freeman & Co., New York.
- Backus, G. & Mulcahy, M., 1976a. Moment tensors and other phenomenological descriptions of seismic sources – I. Continuous displacements, *Geophys. J. R. astr. Soc.*, **46**, 341–361.
- Backus, G. & Mulcahy, M., 1976b. Moment tensors and other phenomenological descriptions of seismic sources – II. Discontinuous displacements, *Geophys. J. R. astr. Soc.*, **47**, 301–329.
- Ben-Menahem, A. & Singh, S.J., 1968a. Eigenvector expansion of Green's dyads with applications to geophysical theory, *Geophys. J. R. astr. Soc.*, **16**, 417–452.
- Ben-Menahem, A. & Singh, S.J., 1968b. Multipolar elastic fields in a layered half space, *Bull. seism. Soc. Am.*, **58**, 1519–1572.
- Chinnery, M.A., 1961. The deformation of ground around surface faults, *Bull. seism. Soc. Am.*, **51**, 355–372.
- Chinnery, M.A., 1963. The stress changes that accompany strike-slip faulting, *Bull. seism. Soc. Am.*, **53**, 921–932.
- Fernández, J. & Rundle, J.B., 1994. Gravity changes and deformation due to a magmatic intrusion in a two-layered crustal model, *J. geophys. Res.*, **99**, 2737–2746.
- Fernández, J., Tiampo, K.F. & Rundle, J.B., 2001. Viscoelastic displacement and gravity changes due to point magmatic intrusions in a gravitational layered solid earth, *Geophys. J. Int.*, **146**, 155–170.
- Folch, A., Fernández, J., Rundle, J.B. & Martí, J., 2000. Ground deformation in a viscoelastic medium composed of a layer overlying a half-space: a comparison between point and extended sources, *Geophys. J. Int.*, **140**, 37–50.
- Foulger, G.R., Jahn, C.-H., Seeber, G., Einarsson, P., Julian, B.R. & Heki, K., 1992. Post-rifting stress relaxation at the divergent plate boundary in Northeast Iceland, *Nature*, **358**, 488–490.
- Fukahata, Y. & Matsu'ura, M., 2005. General expressions for internal deformation fields due to a dislocation source in a multilayered elastic half-space, *Geophys. J. Int.*, **161**, 507–521.
- Fukahata, Y. & Matsu'ura, M., 2006. Quasi-static internal deformation due to a dislocation source in a multilayered elastic/viscoelastic half-space and an equivalence theorem, *Geophys. J. Int.*, **166**, 418–434.

- Hashimoto, C. & Matsu'ura, M., 2000. 3-D physical modeling of stress accumulation and release processes at transcurrent plate boundaries, *Pure appl. Geophys.*, **157**, 2125–2147.
- Hashimoto, C., Fukui, K. & Matsu'ura, M., 2004. 3-D modeling of plate interfaces and numerical simulation of long-term crustal deformation in and around Japan, *Pure appl. Geophys.*, **161**, 2053–2068.
- Haskell, N.A., 1953. The dispersion of surface waves on a multilayered medium, *Bull. seism. Soc. Am.*, **43**, 17–34.
- He, Y.-M., Wang, W.-M. & Yao, Z.-X., 2003a. Static deformation due to shear and tensile faults in a layered half-space, *Bull. seism. Soc. Am.*, **93**, 2253–2263.
- He, Y.-M., Wang, W.-M. & Yao, Z.-X., 2003b. Static displacement due to seismic moment tensor sources in a layered half-space, *Chin. Phys. Lett.*, **20**, 1397–1400.
- Hofton, M.A. & Foulger, G.R., 1996. Postrifting anelastic deformation around the spreading plate boundary, north Iceland 2. Implications of the model derived from the 1987–1992 deformation field, *J. geophys. Res.*, **101**, 25423–25436.
- Hofton, M.A., Rundle, J.B. & Foulger, G.R., 1995. Horizontal surface deformation due to dike emplacement in an elastic-gravitational layer overlying a viscoelastic-gravitational half-space, *J. geophys. Res.*, **100**, 6329–6338.
- Iwasaki, T. & Matsu'ura, M., 1981. Quasi-static strain and tilt due to faulting in a layered half-space with an intervenient viscoelastic layer, *J. Phys. Earth*, **29**, 499–518.
- Iwasaki, T. & Matsu'ura, M., 1982. Quasi-static crustal deformations due to a surface load: rheological structure of the Earth's crust and upper mantle, *J. Phys. Earth*, **30**, 469–508.
- Iwasaki, T. & Sato, R., 1979. Strain field in a semi-infinite medium due to an inclined rectangular fault, *J. Phys. Earth*, **27**, 285–314.
- Jovanovich, D.B., Husseini, M.I. & Chinnery, M.A., 1974a. Elastic dislocations in a layered half-space – I. Basic theory and numerical methods, *Geophys. J. R. astr. Soc.*, **39**, 205–217.
- Jovanovich, D.B., Husseini, M.I. & Chinnery, M.A., 1974b. Elastic dislocations in a layered half-space – II. The point source, *Geophys. J. R. astr. Soc.*, **39**, 219–239.
- Kennett, B.L.N., 1983. *Seismic Wave Propagation in Stratified Media*, Cambridge University Press, Cambridge.
- Lee, E.H., 1955. Stress analysis in visco-elastic bodies, *Q. Appl. Math.*, **13**, 183–190.
- Ma, X.Q. & Kusznir, N.J., 1992. 3-D subsurface displacement and strain fields for faults and fault arrays in a layered elastic half space, *Geophys. J. Int.*, **111**, 542–558.
- Mansinha, L. & Smylie, D.E., 1971. The displacement fields of inclined faults, *Bull. seism. Soc. Am.*, **61**, 1433–1440.
- Maruyama, T., 1964. Static elastic dislocations in an infinite and semi-infinite medium, *Bull. Earthq. Res. Inst., Univ. Tokyo*, **42**, 289–368.
- Matsu'ura, M. & Iwasaki, T., 1983. Study on coseismic and postseismic crustal movements associated with the 1923 Kanto earthquake, *Tectonophysics*, **97**, 201–215.
- Matsu'ura, M. & Sato, R., 1975. Static deformations due to the fault spreading over several layers in a multi-layered medium. Part II: strain and tilt, *J. Phys. Earth*, **23**, 1–29.
- Matsu'ura, M. & Sato, T., 1989. A dislocation model for the earthquake cycle at convergent plate boundaries, *Geophys. J. Int.*, **96**, 23–32.
- Matsu'ura, M. & Sato T., 1997. Loading mechanism and scaling relations of large interplate earthquakes, *Tectonophysics*, **277**, 189–198.
- Matsu'ura, M. & Tanimoto, T., 1980. Quasi-static deformations due to an inclined, rectangular fault in a viscoelastic half-space, *J. Phys. Earth*, **28**, 103–118.
- Matsu'ura, M., Tanimoto, T. & Iwasaki, T., 1981. Quasi-static displacements due to faulting in a layered half-space with an intervenient viscoelastic layer, *J. Phys. Earth*, **29**, 23–54.
- McConnell, R.K., 1965. Isostatic adjustment in a layered Earth, *J. geophys. Res.*, **20**, 5171–5188.
- Nur, A. & Mavko, G., 1974. Postseismic viscoelastic rebound, *Science*, **183**, 204–206.
- Okada, Y., 1992. Internal deformation due to shear and tensile faults in a half-space, *Bull. seism. Soc. Am.*, **82**, 1018–1040.
- Pan, E., 1997. Static Green's functions in multilayered half spaces, *Appl. Math. Modell.*, **21**, 509–521.
- Press, F., 1965. Displacements, strains and tilts at teleseismic distances, *J. geophys. Res.*, **70**, 2395–2412.
- Radok, J.R.M., 1957. Visco-elastic stress analysis, *Q. Appl. Math.*, **15**, 198–202.
- Roth, F., 1990. Subsurface deformations in a layered elastic half-space, *Geophys. J. Int.*, **103**, 147–155.
- Roth, F., 1993. Deformations in a layered crust due to a system of cracks— modeling the effect of dike injections or dilatancy, *J. geophys. Res.*, **98**, 4543–4551.
- Rundle, J.B., 1978. Viscoelastic crustal deformation by finite quasi-static sources, *J. geophys. Res.*, **83**, 5937–5945.
- Rundle, J.B., 1980. Static elastic-gravitational deformation of a layered half-space by point couple sources, *J. geophys. Res.*, **85**, 5355–5363.
- Rundle, J.B., 1982a. Viscoelastic-gravitational deformation by a rectangular thrust fault in a layered earth, *J. geophys. Res.*, **87**, 7787–7796.
- Rundle, J.B., 1982b. Deformation, gravity, and potential changes due to volcanic loading of the crust, *J. geophys. Res.*, **87**, 10 729–10 744.
- Sato, R., 1971. Crustal deformation due to dislocation in a multi-layered medium, *J. Phys. Earth*, **19**, 31–46.
- Sato, R. & Matsu'ura, M., 1973. Static deformations due to the fault spreading over several layers in a multi-layered medium. Part I: Displacement, *J. Phys. Earth*, **21**, 227–249.
- Sato, R. & Matsu'ura, M., 1974. Strains and tilts on the surface of a semi-infinite medium, *J. Phys. Earth*, **22**, 213–221.
- Sato, T. & Matsu'ura, M., 1992. Cyclic crustal movement, steady uplift of marine terraces, and evolution of the island arc-trench system in southwest Japan, *Geophys. J. Int.*, **111**, 617–629.
- Sato, T. & Matsu'ura, M., 1993. A kinematic model for evolution of island arc-trench systems, *Geophys. J. Int.*, **114**, 512–530.
- Savage, J.C. & Hastie, L.M., 1966. Surface deformation associated with dip-slip faulting, *J. geophys. Res.*, **71**, 4897–4904.
- Savage, J.C. & Prescott, W.H., 1978. Asthenosphere readjustment and earthquake cycle, *J. geophys. Res.*, **83**, 3369–3376.
- Singh, S.J., 1970. Static deformation of a multilayered half-space by internal sources, *J. geophys. Res.*, **75**, 3257–3263.
- Steketee, J.A., 1958a. On Volterra's dislocations in a semi-infinite elastic medium, *Can. J. Phys.*, **36**, 192–205.
- Steketee, J.A., 1958b. Some geophysical application of the elasticity theory of dislocations, *Can. J. Phys.*, **36**, 1168–1198.
- Stokes, G.G., 1849. On the dynamical theory of diffraction, *Trans. Camb. Phil. Soc.*, **9**, 1.
- Takeuchi, H., 1959. General solutions of equations of some geophysical importance, *Bull. seism. Soc. Am.*, **49**, 273–283.
- Thatcher W. & Rundle, J.B., 1979. A model for the earthquake cycle in underthrust zones, *J. geophys. Res.*, **84**, 5540–5556.
- Thatcher, W. & Rundle, J.B., 1984. A viscoelastic coupling model for the cyclic deformation due to periodically repeated earthquakes at subduction zones, *J. geophys. Res.*, **89**, 7631–7640.
- Thomson, W.T., 1950. Transmission of elastic waves through a stratified medium, *J. Appl. Phys.*, **21**, 89–93.
- Wang, R., 1999. A simple orthonormalization method for stable and efficient computation of Green's functions, *Bull. seism. Soc. Am.*, **89**, 733–741.
- Wang, R., Lorenzo-Martin, F. & Roth, F., 2006. PSGRN/PSCMP—a new code for calculating co- and post-seismic deformation, geoid and gravity changes based on the viscoelastic-gravitational dislocation theory, *Comput. Geosci.*, **32**, 527–541.
- Xie, X.-B. & Yao, Z.-X., 1989. A generalized reflection-transmission coefficient matrix method to calculate static displacement field of a stratified half-space by dislocation source, *Chinese J. Geophys.*, **32**, 270–280.
- Zhu, L. & Rivera, L.A., 2002. A note on the dynamic and static displacements from a point source in multilayered media, *Geophys. J. Int.*, **148**, 619–627.

**APPENDIX A: EXPRESSIONS FOR STRUCTURE-DEPENDENT MATRICES**

In this Appendix, we show the explicit expressions for the structure-dependent matrices used in Section 3 of the text. The structure-dependent matrices are independent of source properties, and so they are the same as those for shear faulting in Fukahata & Matsu'ura (2005).

The explicit expressions for  $\mathbf{E}_j(z)$  and  $\mathbf{E}'_j(z)$ , which are the  $z$ -dependent parts of the deformation matrices  $\mathbf{Y}^g(z; j)$  and  $\mathbf{Y}'^g(z; j)$ , are given by

$$\left\{ \begin{array}{l} \mathbf{E}_{j(\neq n)}(z) = \begin{bmatrix} c(z) & -\gamma_j z \xi c(z) & s(z) & -\gamma_j z \xi s(z) \\ s(z) & (2 - \gamma_j)c(z) - \gamma_j z \xi s(z) & c(z) & (2 - \gamma_j)s(z) - \gamma_j z \xi c(z) \\ s(z) & (1 - \gamma_j)c(z) - \gamma_j z \xi s(z) & c(z) & (1 - \gamma_j)s(z) - \gamma_j z \xi c(z) \\ c(z) & s(z) - \gamma_j z \xi c(z) & s(z) & c(z) - \gamma_j z \xi s(z) \end{bmatrix}, \\ \mathbf{E}'_{j(\neq n)}(z) = \begin{bmatrix} c(z) & s(z) \\ s(z) & c(z) \end{bmatrix} \end{array} \right. \quad (\text{A1})$$

$$\mathbf{E}_n(z) = e^{-z\xi} \begin{pmatrix} 1 & 0 & 0 & \gamma_n z \xi \\ 0 & 2 - \gamma_n + \gamma_n z \xi & 1 & 0 \\ 0 & 1 - \gamma_n + \gamma_n z \xi & 1 & 0 \\ 1 & 0 & 0 & 1 + \gamma_n z \xi \end{pmatrix}, \quad \mathbf{E}'_n(z) = e^{-z\xi} \begin{pmatrix} 1 & 0 \\ 0 & 1 \end{pmatrix}, \quad (\text{A2})$$

$$\mathbf{E}_j(0) = \begin{pmatrix} 1 & 0 & 0 & 0 \\ 0 & 2 - \gamma_j & 1 & 0 \\ 0 & 1 - \gamma_j & 1 & 0 \\ 1 & 0 & 0 & 1 \end{pmatrix}, \quad \mathbf{E}_j^{-1}(0) = \begin{pmatrix} 1 & 0 & 0 & 0 \\ 0 & 1 & -1 & 0 \\ 0 & -1 + \gamma_j & 2 - \gamma_j & 0 \\ -1 & 0 & 0 & 1 \end{pmatrix}, \quad (\text{A3})$$

with

$$s(z) = \sinh(z\xi), \quad c(z) = \cosh(z\xi) \quad (\text{A4})$$

and

$$\gamma_j = (3K_j + \mu_j)/(3K_j + 4\mu_j), \quad (\text{A5})$$

where  $K_j$  and  $\mu_j$  are the bulk modulus and the rigidity of the  $j$ th layer, respectively.

The explicit expression for the down-going expression  $\mathbf{F}_j(z)$  of the generalized propagator matrices defined in eq. (54) of the text is given by

$$\mathbf{F}_j(z) = \begin{bmatrix} c(z) + \gamma_j z \xi s(z) & (\gamma_j - 1)s(z) - \gamma_j z \xi c(z) & (2 - \gamma_j)s(z) + \gamma_j z \xi c(z) & -\gamma_j z \xi s(z) \\ (\gamma_j - 1)s(z) + \gamma_j z \xi c(z) & c(z) - \gamma_j z \xi s(z) & \gamma_j z \xi s(z) & (2 - \gamma_j)s(z) - \gamma_j z \xi c(z) \\ \gamma_j s(z) + \gamma_j z \xi c(z) & -\gamma_j z \xi s(z) & c(z) + \gamma_j z \xi s(z) & (1 - \gamma_j)s(z) - \gamma_j z \xi c(z) \\ \gamma_j z \xi s(z) & \gamma_j s(z) - \gamma_j z \xi c(z) & (1 - \gamma_j)s(z) + \gamma_j z \xi c(z) & c(z) - \gamma_j z \xi s(z) \end{bmatrix}. \quad (\text{A6})$$

The explicit expressions for the other structure-dependent matrices are given by

$$\mathbf{G} = \begin{pmatrix} 1 & 0 & 0 & 0 \\ 0 & 1 & 0 & 0 \\ 0 & 0 & 1 & 0 \\ 0 & \rho_1 g / 2\mu_1 \xi & 0 & 1 \end{pmatrix}, \quad \mathbf{G}^{-1} = \begin{pmatrix} 1 & 0 & 0 & 0 \\ 0 & 1 & 0 & 0 \\ 0 & 0 & 1 & 0 \\ 0 & -\rho_1 g / 2\mu_1 \xi & 0 & 1 \end{pmatrix}, \quad (\text{A7})$$

$$\mathbf{D}_j = \begin{pmatrix} 1 & 0 & 0 & 0 \\ 0 & 1 & 0 & 0 \\ 0 & 0 & \mu_j / \mu_{j+1} & 0 \\ 0 & 0 & 0 & \mu_j / \mu_{j+1} \end{pmatrix}, \quad \mathbf{D}'_j = \begin{pmatrix} 1 & 0 \\ 0 & \mu_j / \mu_{j+1} \end{pmatrix}, \quad (\text{A8})$$

where  $\rho_1$  is the density of the surface layer, and  $g$  is the acceleration of gravity at the Earth's surface.